DEVELOPMENT OF REDUCED GRAPHENE OXIDE/ HIGH DENSITY POLYETHYLENE (RGO/ HDPE) HIGH PERFORMANCE NANOCOMPOSITES

LEONG WENG WOH

A project report submitted in partial fulfilment of the requirements for the award of the degree of Bachelor of Engineering (Hons.) Petrochemical Engineering

Faculty of Engineering and Green Technology
Universiti Tunku Abdul Rahman

January 2015

DECLARATION

I hereby declare that this project report is based on my original work except for citations and quotations which have been duty acknowledged. I also declare that it has not been previously and concurrently submitted for any other degree or award at UTAR or other institutions.

Signature : _____

Name : LEONG WENG WOH

ID No. : 10AGB03095

Date : _____

APPROVAL FOR SUBMISSION

I certify that this project report entitled **"DEVELOPMENT OF REDUCED GRAPHENE OXIDE/ HIGH DENSITY POLYETHYLENE (RGO/ HDPE) HIGH PERFORMANCE NANOCOMPOSITES"** was prepared by **LEONG WENG WOH** has met the requirement standard for submission in partial fulfilment of the requirements for the award of Bachelor of Engineering (Hons) Petrochemical Engineering at Universiti Tunku Abdul Rahman.

Approved by,

Signature : _____

Supervisor : Dr. Yamuna a/p Munusamy

Date : _____

Specially dedicated to
My beloved grandmother and parents

ACKNOWLEDGEMENTS

I would like to thank everyone who had contributed to the successful completion of this project. I would like to express my gratitude to my research supervisor, Dr. Yamuna a/p Munusamy for her invaluable advice, guidance and her enormous patience throughout the development of this research. In additions, I also would like to express my gratitude to Dr. Mathialagan a/l Muniyadi for his support and guidance throughout the whole project.

In addition, I would like to express my gratitude to my loving parents and friends who had helped and give me encouragement. Special dedication is given to my seniors who assisted me throughout the research. Their support and guidance allow this research to be completed smoothly.

DEVELOPMENT OF REDUCED GRAPHENE OXIDE/ HIGH DENSITY POLYETHYLENE (RGO/ HDPE) HIGH PERFORMANCE NANOCOMPOSITES

ABSTRACT

In this research, graphene oxide (GO) was synthesized from graphite nanofiber (GNF) using the conventional Hummer methods. The reduced graphene oxide (rGO) was successfully reduced using the chemical reduction by formic acid which was a green, metal free and environmentally friendly reduction method. Different loading of rGO; 0.05 wt%, 0.10 wt%, 0.15 wt% and 0.20 wt% respectively was incorporated into the high density polyethylene (HDPE) to produce HDPE/rGO nanocomposite through melt intercalation method. Characterization test such as Fourier Transform Infrared Spectroscopy (FTIR) was conducted on GO and rGO for the confirmation on the removal of oxygen contained functional group in rGO. For HDPE/rGO nanocomposites, FTIR was carried out to determine the presence of rGO in the nanocomposites while preserving the important peaks of HDPE. Further testing such as Differential Scanning Calorimetry (DSC) and Melt Flow Index (MFI) was done on pure HDPE and HDPE/rGO nanocomposites. DSC was conducted to measure the melting point (T_m), recrystallization temperature (T_c) and crystallinity of nanocomposites. The results showed there were increased in the crystallinity. There was slightly increased in thermal stability. MFI was conducted to determine the flow measurement and viscosity of nanocomposite when in molten state. The MFI values increased which indicated the decrease in viscosity as well. Performance test such as Impact and Tensile test was conducted to determine the mechanical properties of nanocomposite. Impact test showed increment in impact strength when there was increased in rGO loading. The tensile test showed that the optimum loadings for rGO incorporated to HDPE was 0.15 wt% which showed increased in both e-modulus and tensile strength and decreased in elongation at break. The overall test showed that there was increased in thermal and mechanical properties of HDPE/rGO

nanocomposite. Field Emission Scanning Electron Microscopy (FESEM) was carried out to determine the surface morphology and filler matrix interaction of HDPE/rGO nanocomposites fracture composite. The surface morphology became rougher when the rGO loadings increased. Agglomeration was observed which might reduce the tensile strength of nanocomposite. Good dispersion of filler matrix interfacial interaction for HDPE/rGO 0.15 wt% nanocomposite was observed in SEM. Therefore, incorporation of rGO into HDPE produced a new HDPE/rGO nanocomposite with enhanced properties such as thermal and mechanical properties.

Keywords: reduced Graphene Oxide (rGO), High density Polyethylene (HDPE), Chemical reduction, Formic acid.

TABLE OF CONTENTS

LIST OF TABLES

LIST OF FIGURES

LIST OF SYMBOLS / ABBREVIATIONS

%	Percentage
°C	Degree Celsius
°F	Degree Fahrenheit
Atm	Atmospheric Pressure
g	Gram
g/10 min	Grams per 10 minutes
J	Joule
kg	Kilogram
kJ/m^2	Kilo Joule per metre square
ml	Millilitre
ml/min	Millilitre per minutes
mm	Millimetre
mm/min	Millimetre per minutes
MPa	Megapascal
N	Newton
Nm	Newton metre
rpm	Revolution per minutes
µL	Microlitre
wt%	Weight percentage
ΔH_m	Melting heat, J/g
ΔH_{100}	Melting heat for 100 % crystalline HDPE, 293.6 J/g
0D	zero-dimensional
1D	one-dimensional
2D	two-dimensional
3D	three-dimensional
300X	Magnification of 300X
500X	Magnification of 500X

1000X	Magnification of 1000X
ABS	Acrylonitrile butadiene styrene
C	Carbon
CB	Carbon Black
CNTs	Carbon Nanotubes
CVD	Chemical Vapour Deposition
C–O Stretch	Alkoxy groups
C–O–C Stretch	Epoxy groups
C=C Stretch	Aromatic C=C bonds
C=O Stretch	Carbonyls (general) groups
$CH_2=CH_2$	Ethylene
C_7H_{16}	Heptane
DI	Deionized Water
DSC	Deferential Scanning Calorimetry
DWCNT	Double-Wall Carbon Nanotubes
EG	Exfoliated Graphite
EPR-g-MA	Maleated Ethylene/Propylene Elastomers
FDA	Food and Drug Administration
FESEM	Field Emission Scanning Electron Microscopy
FTIR	Fourier Transform Infrared Spectroscopy
GNF	Graphite Nanofiber
GO	Graphene Oxide
H	Hydrogen
HCl	Hydrochloric Acid
HDPE	High Density Polyethylene
HDPE/BF	High Density Polyethylene/Bamboo Flour
HDPE/rGO	High Density Polyethylene/reduced Graphene Oxide
HDPE/rGO 0.05 wt%	HDPE/rGO nanocomposite with 0.05 weight percentage
HDPE/rGO 0.10 wt%	HDPE/rGO nanocomposite with 0.10 weight percentage
HDPE/rGO 0.15 wt%	HDPE/rGO nanocomposite with 0.15 weight percentage
HDPE/rGO 0.20 wt%	HDPE/rGO nanocomposite with 0.20 weight percentage
HMWPE	High Molecular Weight Polyethylene

HNO_3	Nitric Acid
H_2O_2	Hydrogen Peroxide
H_2SO_4	Sulphuric Acid
$KClO_3$	Potassium Chlorate
KBr	Potassium Bromide
$KMnO_4$	Potassium Permanganate
LDPE	Low Density Polyethylene
LLDPE	Linear Low Density Polyethylene
MAPE	Maleic Anhydride Grafted HDPE
MDPE	Medium Density Polyethylene
Mn_2O_7	Dimanganeseheptoxide
MWNT	Multi-walled Carbon Nanotubes
$NaNO_3$	Sodium Nitrate
nm	Nanometre
O–H Stretch	Alcohols, Phenols, Hydroxyl groups
O_2	Oxygen
PE	Polyethylene
PE-g-MA	Maleated Polyethylene
PE-WAX	Ultra Low Molecular Weight Polyethylene
PMMA	Poly (Methyl Methacrylate)
PMMA/$Ce(OH)_3$, Pr_2O_3/NanoG	Poly (Methyl Methacrylate)/Graphite Nanosheet
rGO	reduced Graphene Oxide
SF	Sisal Fiber
TGA	Thermogravimetric Analysis
$TiCl_4$	Titanium Chloride
T_M	Melting point, ˚C
T_C	Recrystallization temperature, ˚C
UHMWPE	Ultra High Molecular Weight Polyethylene
ULMWPE	Ultra Low Molecular Weight Polyethylene
VLDPE	Very Low Density Polyethylene
W_P	Weight fraction of polymer in sample
X_C^M	Crystallinity, %

LIST OF APPENDICES

CHAPTER 1

INTRODUCTION

1.1 Background

In recent years, automotive industry is on the edge of transformation and the development of polymer composites shows an important character in the revolution of automotive industry. The 21st century will offer automobiles with fundamentally enhanced and improved safety, wellbeing and sustainability attributes (Fisher et al., 2004). In 1950, the revolution of plastics in automotive industry started when thermoplastics made their presentation, beginning with Acrylonitrile butadiene styrene (ABS) and going ahead to polyamide, polyacetal and also polycarbonate together with the introduction of composites, alloys and blends or mixed of different polymers (Szeteiová, 2010). The progressing advancement of the development had led to drastically expansion in the utilization of the high performance polymers.

Initially, plastics were special as they offered great mechanical properties combined with excellent appearance. They incorporate a widespread selection of well-designed polymeric composites which display a huge series of desired possessions. Plastics are lightweight, strong and durable as well as heat, chemical and corrosion resistance. Besides, they are excellent thermal and electrical insulators which enable them to be made thermally and electrically conductive (Fisher et al., 2004).

The utilization of plastic components in the automotive industry has been expanding throughout the last decades. These days, the application of plastics are basically used in making automobiles more energy efficient and vitality productive by diminishing the weight

or reduced the mass of car body, together with providing strength, toughness, durability, flexibility in design, resiliency and high performance at low cost (Szeteiová, 2010).

Since plastics are flexible and lightweight, they consist of structure > 50 % of the volume for the material used in the new automobiles industry. The applications of both thermosets and thermoplastics in traveller vehicles have developed from around 30 kilograms every automobile in 1970 to around 150 kg today (Fisher et al., 2004). In North America, an average size automobile fabricated is around 10-12 % plastics by the overall weight whereby the usage of volume for the material used was larger. Thus, the automotive industry nowadays is very competitive in the market and the demand of plastic or polymer will be much greater than ever due to the competitive challenges in the industry. Research and development of polymers in this field will continue in the next decade in order to help engineers and designers to have a better innovation and enhance performance in the automotive industry.

In this study, high density polyethylene (HDPE) was being studied. HDPE was produced when ethylene was catalyzed by an organometallic compound under moderate pressure condition which is around 10 to 80 atm in the presence of a Ziegler-Natta or inorganic catalyst (Essentialchemicalindustry.org, 2014). It has high tensile strength, lightweight, excellent chemical and impact resistance (Upcinc.com, 2010). Most of the high density polyethylene (HDPE) was used in the manufacturing of containers such as bottles, jugs in food packaging industry (Scifun.com, 2012). In automotive industry, high density polyethylene (HDPE) was applied and used in packaging, electrical insulation, glass reinforced for the car bodies whereby the strength and aesthetics are important in the automotive industry (Szeteiová, 2010).

Graphene and graphene based polymer have attracted great interest and attention for their unique and excellent properties such as mechanical, thermal, electrical and optical properties. It signifies a totally new category of promising material with only one atom thick and offers a new pathway into low dimensional physics science (Sekhar, 2015). Examination and research work with respect to graphene was quickly expanding in scientific materials, solid-state physical science and condensed material physical science. Graphene oxide (GO) is a special material and it is a single monomolecular layer of graphite with various oxygen-containing functionalities, for examples hydroxyl, epoxy, carbonyl and carboxyl groups.

Basically, a key subject in the exploration and application of GO was being reduced whereby the structure and properties of graphene were partially restored. Different properties of reduced graphene oxide (rGO) can be produced from different reduction processes or methodologies, which thusly influence the final performance of the materials composed of reduced graphene oxide (rGO) (Pei and Cheng, 2012). GO and rGO have been utilized as a part of nanocomposite materials, polymer composite materials, biomedical applications, energy storage, catalysis and as a surfactant with some overlaps between these fields (Sekhar, 2015).

In the present work, reduced graphene oxide (rGO) will be introduced as filler to the HDPE to form a new nanocomposite with enhanced properties. The effects of composition and filler type on morphology characterization of composite, thermal and mechanical properties have been examined (Thongruang, 2002). High performance high density polyethylene/reduced graphene oxide (HDPE/rGO) nanocomposite will be produced through melt intercalation technique. The reduced graphene oxide (rGO) will be incorporated into high density polyethylene (HDPE) to increase its thermal properties and mechanical properties. Thus, in this research, the aim is to produce a new nanocomposite, high density polyethylene/reduced graphene oxide (HDPE/rGO) will have a large potential to be used in automobile applications and their industry.

1.2 Problem Statement

In these years, polymer nanocomposites have greatly attracted interest and attention in different industry (Lau et al., 2011). These new classes of polymer nanocomposites material is capable to enhance and provide significant improvements in the combined mechanical and thermal properties. Therefore, the incorporation of graphene fillers into high density polyethylene (HDPE) has been done in various studies to enhance and improve its mechanical properties, electrical properties and thermal stability.

The main advantage of high density polyethylene (HDPE) as polymer matrix is due to its excellent properties such as chemically resistant, impact resistant, electrical resistance and economically or low cost (Prospector.com, 2014). However, there are also some disadvantages such as the use of HDPE as polymer matrix in load bearing uses was limited due to the low stiffness and strength. The mechanical properties of the composites still greatly lower due to the micron-sized reinforcement or agglomeration, low thermal properties and poor filler matrix interaction in the composite (Prospector.com, 2014).

In additions, it is discovered that the basic or essential physical science and chemistry regarding on the characteristic and property improvement through the addition of nanocomposites was still ineffectively comprehended (Lau et al., 2011). Thus, there is still opportunity to get better in this exploration for improvement in this research area. The effect of composition and filler type on morphology characterization of composite, thermal and mechanical properties will be discussed in this paper (Thongruang, 2002). Therefore, the incorporation of reduced graphene oxide (rGO) filler to high density polyethylene (HDPE) is expected to increase the thermal stability, mechanical and thermal properties. This enhancement is expected to happen due to the physical properties of reduced graphene oxide (rGO) itself and good filler matrix interaction.

1.3 Research Objectives and Aims

The objectives of this study are:

- To formulate reduced Graphene Oxide (rGO).
- To prepare reduced Graphene Oxide/High Density Polyethylene (rGO/HDPE) nanocomposite through melt intercalation technique.
- To study the effect of reduced Graphene Oxide (rGO) on the mechanical, thermal, processing properties of High Density Polyethylene (HDPE).

CHAPTER 2

LITERATURE REVIEW

2.1 Overview of High Density Polyethylene (HDPE)

Polyethylene (PE) was a thermoplastic polymer which consist of long chains of the monomer known as ethylene (CH_2=CH_2) with double bond in between each other (Azeem, 2011; Scifun.org, 2012). It contains only the chemical elements such as carbon (C) and hydrogen (H). Figure 2.1 showed the chemical formula of ethylene which is $(-CH_2-CH_2)_n$ whereby the *n* is the number of repeating units.

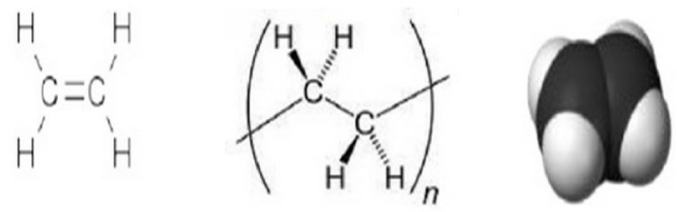

Figure 2.1: Chemical and Structural Formula of Ethylene (Azeem, 2011)

Polyethylene can be produced through polymerization of ethylene. Generally, it can be created through four types of polymerization which were radical, addition of anionic, ion coordination and addition of cationic polymerization (Peacock, 2000). Polyethylene consists of good properties such as water, acid and base resistant. Applications of PE included packaging films, drinking bottles and glasses, pipes and insulation for wire and cable.

High density polyethylene (HDPE) is a linear, semi-crystalline homopolymer of ethylene. The schematic diagram of HDPE was showed in Figure 2.2. It was mostly made from petroleum. Generally, HDPE has a linear structure with low degree of branching which lead to higher density and more crystalline structure when compared to low density polyethylene (LDPE) (Icis.com, 2007; Prospector.com, 2014). Thus, with these properties, it made HDPE to have greater intermolecular forces, good tensile and high impact strength. It was also more rigid and high stiffness but less transparent than LDPE due to higher crystalline properties. In fact, HDPE is actually four times stronger than LDPE (Azeem, 2011).

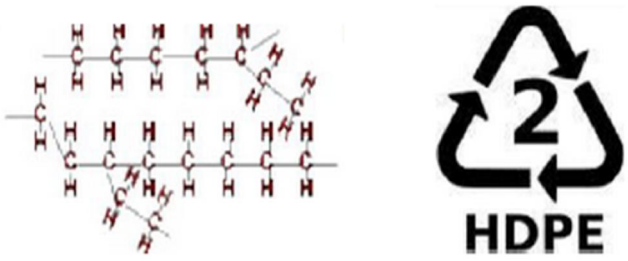

Figure 2.2: Schematic Diagram of HDPE (Azeem, 2011)

Besides, the properties of HDPE are mostly measured by its density and molecular weight distributions. HDPE consists of other good properties such as chemical resistant, resistant to abrasion, corrosion, stains and odours, insoluble in organic solvents, high durability up to 180°F, easy to clean, antioxidant and disinfect, easily extruded or pressed, good processability and FDA approved for food handling and processing (Azeem, 2011; Prospector.com, 2014; Tapplastics.com, 2015).

In current market, HDPE was widely used as food storage containers and bottles due to the rigid nature of HDPE itself. For Entertainment category, almost most of the toys factory-made and sold in the market were all made from HDPE (Bpf.co.uk, 2015). Besides, it also widely used in packaging industries for products such as detergent bottle, milk bottles and garbage containers as HDPE was chemically and physically resistant. In industrial field, HDPE was used as chemical resistant piping systems, water pipes, tanks, laboratory equipment, wire and cable insulation and extrusion coating as well as glass reinforced for the

manufacturing of car HDPE is a disposable thermoformed product which was eco-friendly to the environment (Azeem, 2011; Icis.com, 2007).

2.1.1 Classification of Polyethylene (PE)

Polyethylene (PE) was categorized into few different classes depend on their densities and degree of branching (Peacock, 2000). Generally, the most important polyethylene grades commonly found in the industry used will be linear low, low and high density polyethylene. However, in this research, HDPE will be selected as the polymer material for the whole research. The classification of polyethylene was as shown in table 2.1.

Table 2.1: Classification of Polyethylene (PE) (Plasmat.com, 2008)

	Classification of Polyethylene (PE)
i.	Ultra high molecular weight polyethylene (UHMWPE)
ii.	Ultra low molecular weight polyethylene (ULMWPE or PE-WAX)
iii.	High molecular weight polyethylene (HMWPE)
iv.	High density polyethylene (HDPE)
v.	High density cross-linked polyethylene (HDXLPE)
vi.	Cross-linked polyethylene (PEX or XLPE)
vii.	Medium density polyethylene (MDPE)
viii.	Linear low density polyethylene (LLDPE)
ix.	Low density polyethylene (LDPE)
x.	Very low density polyethylene (VLDPE)

2.2 Production of HDPE

In the year of 1950s, the findings of new catalytic agent in polymerization of ethylene at lower pressure and temperature had increased the possibility of the manufacturing of high density polyethylene (HDPE) in the market. HDPE was mainly produced from ethylene through catalytic process (Prospector.com, 2014). The linearity, degree of short branching and molecular uniformity will formed higher crystallinity and density of the structure (Icis.com, 2007; Peacock, 2000). The increased in density, higher tensile strength, heat distortion temperature, viscosity and chemically resistance of the polymer was mainly due to the increased in crystallinity level.

2.2.1 Type of Catalyst Used

Generally, there were two types of catalyst which were commonly used in the manufacture of high density polyethylene (HDPE). The two catalyst principally used were Ziegler-Natta organometallic catalyst (Titanium compounds with an Aluminium alkyl) or Metallocene catalysts and Phillips-type catalyst which was an inorganic compound (Chromium (VI) oxide on silica) (Azeem, 2011).

2.2.2 Addition Polymerization with a Supported Metal Oxide Catalyst

HDPE can be produced by using an Aluminium-based metal oxide catalyst or metallocene catalyst. The catalytic agent can be utilized in many processes including fixed, fluid, moving bed processes and slurry processes (Azeem, 2011). The polymerization process was carried out at temperature approximately 300°C and pressure 1atm. Monomer of ethylene was fed with a diluting agent such as 2-methylpropane (isobutene) or hexane. In additions, it also can be produced by three types of process through catalytic polymerisation of ethylene which were slurry suspension, solution and gas phase reactors (Azeem, 2011; Icis.com, 2007).

In all these three processes, hydrogen was mixed with the ethylene to control the chain length of the polymer. Alpha-olefin co-monomers such as butene, hexene and octene may be incorporated at low levels in order to modify the polymer's properties (Icis.com, 2007). After polymerization, the polyethylene will be recovered by cooling process or solvent evaporation. The selection of catalyst used was important as it was used to control the class of the desired yield (Icis.com, 2007). Therefore, the well-known Ziegler-Natta and chromium catalysts had been augmented by metallocene catalysts which were claimed to provide improved and enhanced properties (Azeem, 2011).

2.2.3 Coordination Polymerization

Another production method of HDPE was through coordination polymerization. It was carried out under the temperature of 50-75°C and slight pressure. A colloidal suspension was prepared by a catalytic agent through the reaction of an aluminium alkyl and titanium chloride ($TiCl_4$) in heptane (C_7H_{16}). The polyethylene produced will be in the form of powder or granules which was insoluble. When the polymerization finished, the coordination catalyst will be shattered by addition of water or alcohol to the reaction mixture. Eventually, polyethylene will be filtered or centrifuged off, washed and dried (Peacock, 2000).

2.3 Overview of Graphene

Graphene was firstly discovered by two scientists, Andre K. Geim and Konstantin S. Novoselov. Both of them had awarded the Nobel Prize in Physics in year of 2010 for the discovery of graphene (Nobelprize.org, 2010). They had produced, isolated, identified and characterized the graphene well and successfully via a simple mechanical exfoliation method in year 2004. The mechanical exfoliation method was used for the thin films of graphite extraction from its crystal using a scotch tape and shifted it to a silicon substrate (Katz, 2012).

Graphene was the first two-dimensional crystalline single planar sheet of carbon atoms tightly arranged and packed in a hexagonal honeycomb lattice (Geim and Novoselov, 2007). The carbon-carbon distance is approximately 0.142nm (Nobelprize.org, 2010). Generally, it was a sp^2 hybridized carbon atoms and also the simple fundamental element for all graphitic materials such as graphite, carbon nanotube and fullerene (Katz, 2012). Graphene can be enveloped to form fullerenes in 0D, formation of nanotubes in 1D by rolling and 3D graphite through stacking (Allen et al., 2010) as shown in Figure 2.3.

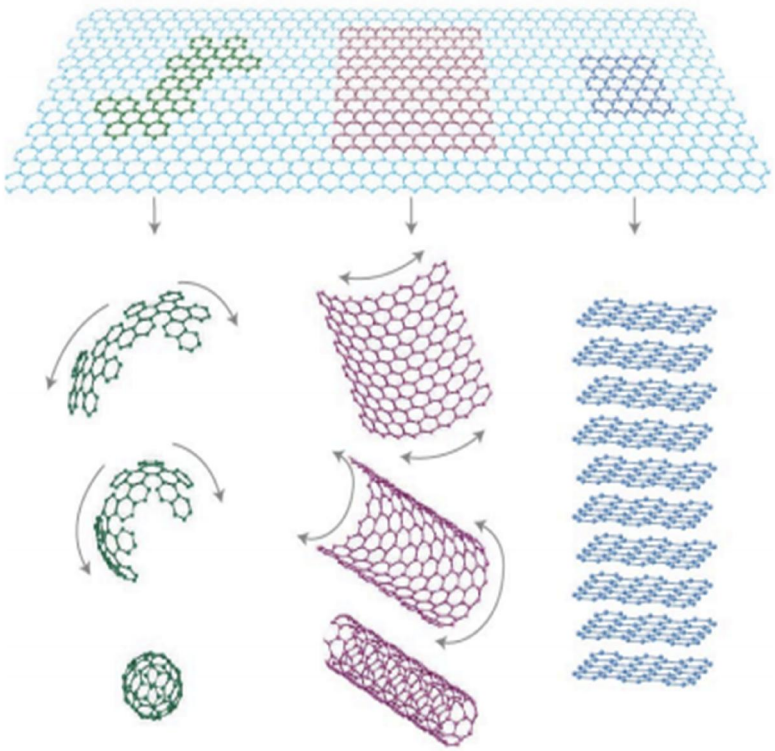

Figure 2.3: 0D Fullrenes; 1D Carbon Nanotube; 2D Graphene; 3D Graphite (Geim and Novoselov, 2007; Nobelprize.org, 2010)

Basically, graphene had attracted great interest and attention for their unique and excellent properties such as high mechanical strength, good thermal properties, unique electrical properties and also great chemical stability (Gao et al., 2010). It signifies a totally new category of promising material with only single atomic layer thick and offers a new pathway into low dimensional physics science (Sekhar, 2015). It was substantially stronger and rigid than steel but can be very durable and stretchable. Thus, it can be used as a flexible

conductor as well. Graphene was a one atom layer thin transparent great conductor along the plane (Nobelprize.org, 2010). The electrons located in *p*–orbitals were on top and bottom of the plane. Then, the *p*–orbitals develop conjugated through the plane and electrons can travel freely across the plane in delocalized orbitals as shown in Figure 2.4.

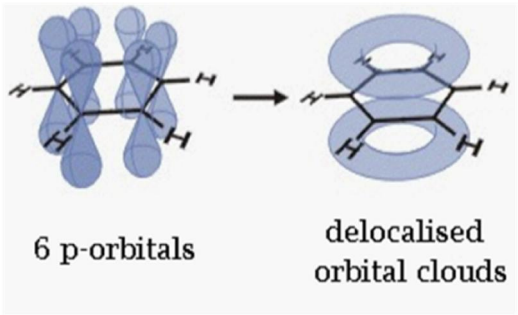

Figure 2.4: Electrons Movement in Delocalized *p*–orbitals (Sekhar, 2015)

In additions, the major purpose for graphene to be widely studied was due to its well-known electrical properties or known as high charge carrier in order to produce electrical technology such as super-capacitor (Brownson et al., 2011; Lu et al., 2013). Besides, the derivative of graphene had also been studied and explored due to its unique properties for further applications. Indeed, it was a huge challenge for researchers in this field to develop a new and effective way for graphene preparations.

2.3.1 Derivates of Graphite

Since graphene had attracted great interest due to its unique properties, it was mainly developed by researchers using several approaches for instance micromechanical exfoliation of graphite, chemical vapour deposition (CVD), chemical reduction of graphene oxide (GO) and exitaxial growth (Gao et al., 2010; Georgakilas et al., 2012).

Among all these approaches, chemical reduction of graphene oxide was more favourable. This was because graphene can be produced from low cost graphite with high yield. Besides, the preparation of graphene from graphene oxide is simple due to highly

hydrophilic properties of graphene oxide which able to form stable aqueous solution to facilitate the synthesis of graphene-based nanocomposites (Zhang et al., 2013). However, there were still some disadvantages in chemical reduction of graphene oxide. An irreversible aggregation through Van der Waals interaction forces and strong *p–p* stacking will be formed by the reduced graphene oxide (rGO) and limits its various potential areas. In order to overcome this technical barrier, attachment of bio-molecular, other small organic molecular or polymer was introduced into the graphene nanosheets.

Another disadvantages was the reductants usually used in chemical reduction of GO was hydrazine, hydrazine derivatives, sodium borohydride and hydroquinone which was highly toxic and hazardous (Zhang et al., 2014). Therefore, a greener, modest, eco-friendly, cheaper in cost and free of metal route was explored by using formic acid for the chemical reduction of graphene oxide (Mitra et al., 2013)

2.4 Overview of Graphene Oxide (GO)

According to Georgakilas et al. (2012), graphene oxide (GO) was a single monolayer of graphene which consist of both aromatic regions (sp^2 carbon atoms) and oxygenated aliphatic regions (sp^3 carbon atoms) that contained epoxy, hydroxyl, carbonyl and carboxyl functional group in randomly distributed order. Generally, the epoxy and hydroxyl functional groups will lie above the graphene whereas the carboxylic functional groups tend to be at the edges of the graphene oxide layers. The schematic model for GO was showed in Figure 2.5.

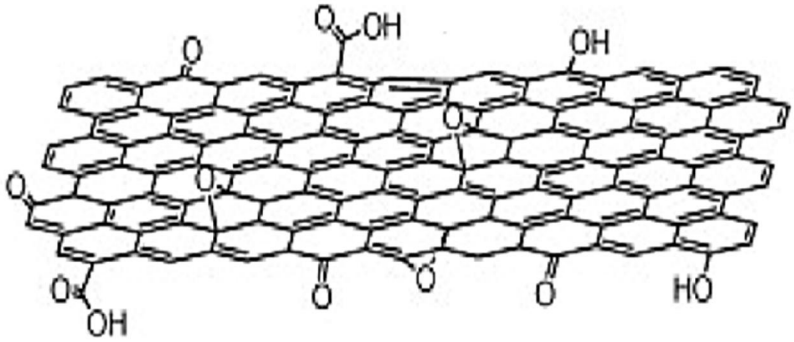

Figure 2.5: Schematic Model of GO (Georgakilas et al., 2012)

Besides, the graphene oxide (GO) tends to be hydrophilic due to the oxygen functional group existed and ready to be exfoliated in water (Park et al., 2009). Researchers had conducted studies and test on its hydrophilicity. In additions, the reactive oxygen functional groups also enable the GO sheets to be chemically linked to other chemicals and substances (Park et al., 2009).

Preparation of GO can be done either by thermal oxidation of graphene or oxidation of graphite with strong acid. A variety of studies had been conducted on application of GO as filler for polymer matrix composites membrane such as polyvinyl alcohol, polyester, polyvinyldiene floride and others (Zhu et al., 2010; Ganesh et al., 2013). Studies and investigations showed increase in mechanical strength, increase in thermal and electrical properties by using graphene oxide (GO) as fillers in polymer matrix (Lu et al., 2013; Zhu et al., 2010). The overview of characteristic of graphite, graphene oxide and reduced graphene oxide was showed in Figure 2.6.

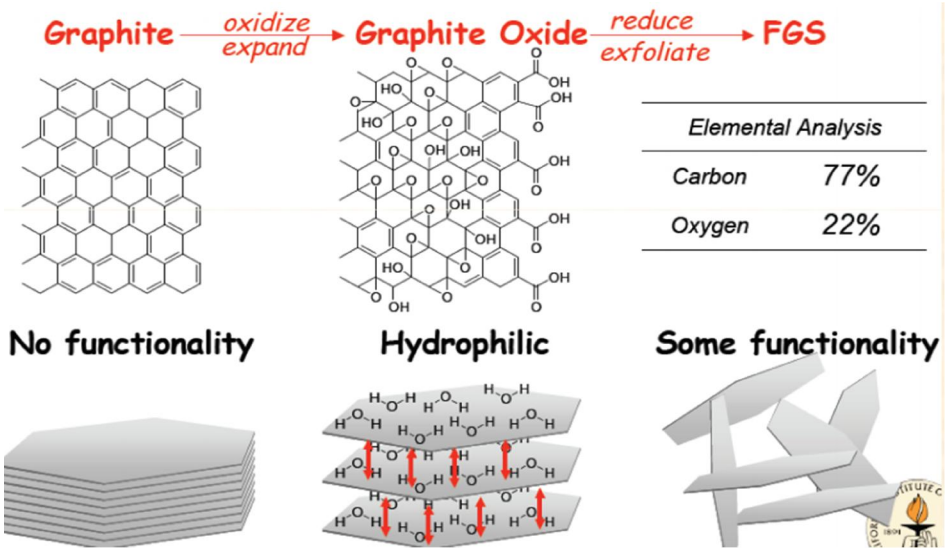

Figure 2.6: Characteristic of Graphite, Graphene Oxide and Reduced Graphene Oxide (Stankovich et al., 2007)

2.5 Preparation of GO

Three main method used to produce GO were Brodie method, Staudenmaier method and Conventional Hummers method. Basically, the preparation of GO included steps like oxidation of graphite or graphite nanofiber (GNF) using strong acid and oxidizer along with a series of hydrolysis, washing, centrifuge and drying (Marcano et al., 2010).

2.5.1 Brodie and Staudenmaier Method

In year of 1985, the first batch of graphene oxide (GO) was prepared by a British chemist named B. C. Brodie when he was investigating the chemistry of graphite (Gao, 2012). A new batch of compound consists of carbon, oxygen and hydrogen was obtained when he added the Potassium chlorate ($KClO_3$) into slurry of graphite in fuming nitric acid (HNO_3) (Marcano et al., 2010). The product was washed and dried at 100 ˚C. After that, it was placed under oxidation treatment until a light yellow substance was formed.

Based on his research and analysis, the empirical formula for the final product obtained was $C_{11}H_4O_5$. Attempts and trials were done by him later on but none of them was successful. Thus, it left a large space to work on and improve for today as his observations and conclusions were limited by the theories and characterization technology available at that time.

The improvement of Brodie's work occurred in 1898 by L. Staudenmaier. There were two major changes introduced by L. Staudenmaier to improve Brodie's work. Staudenmaier modified Brodie's work by adding concentrated sulphuric acid in order to increase the acidity of the mixture. He also added multiple aliquots of potassium chlorate ($KClO_3$) solution into the reaction mixture over the course of reaction. Due to these modifications, the synthesis process was simplified and the GO product obtained can be highly oxidized in a single reaction vessel (Gao, 2012). However, in term of safety, Staudenmaier's method was time consuming as the addition of $KClO_3$ typically lasted over a week. It also hazardous as inert gas was required for the removal of chlorine dioxide evolved from the process. Therefore, an improvement and further modification was needed to develop this oxidation process.

Generally, nitric acid and potassium chlorate was used as the oxidizing agent in both Brodie and Staudenmaier method. Formation of oxygen contained product such as carboxyl, ketone and lactone were normally obtained as the typical result of the reaction (Dreyer et al., 2009).

2.5.2 Conventional Hummers Method

The Hummers method was developed after almost 60 years after Staudenmaier's method by a chemists named Hummers and Offeman in Mellon Institution of Industrial Research. The preparation of graphene oxide started by using a water free combination of sodium nitrate, concentrated sulphuric acid and potassium permanganate which kept under 45˚C for 2 hours. The final product obtained consists of higher degree of oxidation compared to the Staudenmaier's method as shown in Table 2.2.

Table 2.2: Comparison of Staudenmaier GO and Hummers GO in Term of Chemical Compositions (Gao, 2012)

Method	Carbon (wt%)	Oxygen (wt%)	Water (wt%)	Ash (wt%)	C/O atomic ratio
Hummers	47.06	27.92	22.99	1.98	2.25
Staudenmaier	52.11	23.99	22.22	1.90	2.89

However, product produced by Hummers method was usually had an incompletely oxidized graphite core with graphene oxide shells. In order to achieve a higher degree of oxidation, a pre-expansion process was required which was firstly introduced by Kovtyukhova in year of 1999. Thus, a new method for preparation of GO was developed by using the combination of concentrated sulphuric acid (H_2SO_4) and potassium permanganate ($KMnO_4$).

Dreyer et al. (2009) mentioned that the oxidation level obtained was same as the previous method developed by using this method. Nowadays, this was the most popular and common method to synthesize graphite oxide. Scheme 2.1 showed dimanganeseheptoxide (Mn_2O_7) was formed from the reaction of sulphuric acid and potassium permanganate.

$$KMnO_4 + 3H_2SO_4 \rightarrow K^+ + MnO_3^+ + H_3O^+ + 4HSO_4^-$$
$$MnO_3^+ + MnO_4^- \rightarrow Mn_2O_7$$

Scheme 2.1: Formation of Dimanganeseheptoxide (Dreyer et al., 2010)

According to Dreyer et al. (2010), dimanganeseheptoxide was the active species of the oxidant and it possesses *bi* metallic properties. It is more reactive than the monometallic tetraoxide counterpart. Therefore, dimanganeseheptoxide had a higher ability to oxidize graphite to graphene oxide (GO). When the temperature was heated up to 55°C and higher, it tends to detonate and this made it to be temperature sensitive as well.

Based on the conventional Hummers method, a series of chemicals such as concentrated sulphuric acid (H_2SO_4), sodium nitrate ($NaNO_3$), potassium permanganate ($KMnO_4$) and hydrogen peroxide (H_2O_2) was added under different condition and followed by dilution, filtration, washing and drying. The used of H_2O_2 is to terminate the reaction for the post-treatment of graphite oxide. A series of washing was required for the removal of impurities included sulphate ions with the use of hydrochloride acid. The chloride will then dissolve in the distilled water during washing. The solution was centrifuged using a high speed centrifuged machine and washed until the pH of the supernatant reaches around 5 to 7. The final product was then dispersed in deionized water and dried overnight in an oven at around 60-80˚C (Ganesh et al., 2013).

2.6 HDPE Composite

High density polyethylene (HDPE) consists of good properties such as chemically resistance, impact resistance and lightweight. However, it has low thermal properties and low mechanical strength. Based on the research, HDPE composite can enhanced the properties of pure HDPE after introduced filler into it. The filler incorporated into HDPE showed better thermal and mechanical properties (Zhu et al., 2010; Ganesh et al., 2013).

2.6.1 HDPE/Bamboo Flour (HDPE/BF) Composites

HDPE/BF composite improved with two maleated ethylene/propylene elastomers (EPR-g-MA) and one maleated polyethylene (PE-g-MA) was being studied. The HDPE/BF composites morphologies and mechanical properties were investigated.

In majority of polymer filled system, compatibilizers or coupling agents was commonly used to increase and enhance the tensile strength of the polymer through adhesion enhancement between the matrix filler interface. In the research, it showed that the incorporations of PE-g-MA and EPR-g-MA also support interfacial bonding between both HDPE matrix with hydrophobic property and hydrophilic bamboo flour. From the results obtained, it showed that there was improvement in tensile strength of the reinforced HDPE/BF composite (Liu et al., 2008).

2.6.2 Sisal Fiber (SF) Reinforced High Density Polyethylene (HDPE) Composites

In the research, sisal fiber (SF) was incorporated to HDPE and the mechanical properties of the reinforced composites were being studied. According to Zhao et al. (2004), the adding of sisal fiber to HDPE and the interfacial compatibilization with maleic anhydride grafted HDPE (MAPE) showed increment in the mechanical properties of the composites.

In additions, the increment in mechanical properties was also attributed from the improvement of interfacial bonding between the SF and the matrix when it was being compared with simultaneous blending (Zhao et al., 2014). The results obtained showed that there were increments of tensile strength for the reinforced composites which was around 58%, 150% and 257% respectively when the fiber content was increased from 10 wt% to 30 wt%.

2.6.3 High Density Polyethylene/ Textile Fibers Residues Composites

Liu et al. (2008), incorporated textile fibers residues as filler to HDPE to form HDPE/textile fibers residues composites and the mechanical properties were being studied.

In the research, it was found out that there was increased in mechanical properties of composites when sulphuric acid was used in the pretreatment of textile fibers residues. The weight percentage of fibers loading introduced to HDPE was 5 wt% and 10 wt% respectively. The data obtained proved that the HDPE/textile fibers residues composites achieved a better mechanical performance than the original HDPE (Liu et al., 2008).

2.7 Nanofillers

In recent years, nanofillers had attracted great attention and play an important role as it brought high significance to the plastics industry. It can enhance variety of the material properties into which they are incorporated such as thermal, electrical and mechanical properties or fire retardancy of the composite. A good mixture aspect ratio between the nanofiller and matrix will contribute to increase in the composite properties. The advantages of incorporating nanofillers to polymer include improved polymer stiffness, dimension stability, barrier property, electrical conductivity, flame retardancy, heat deflection temperature, impact and tensile strength.

2.8 Types of Nanofillers Commonly Used

2.8.1 Nanoclay

It is a plate-like nanoparticle of natural occurring layered silicates with high aspect ratio and hydrophilic properties. Clay minerals are divided in several categories such as bentonites (Montmorillonites) and hectorites. Bentonites were built up of stacked nanoscopic aluminosilicate plates whereby each plate was around 1nm in height and 1 μm in diameter. It was widely used as filler in plastics and material applications nowadays. The insulation cable used in industry can improved their flame retardancy by adding the organically modified montmorillonites (organoclays). The flame propagation was greatly condensed and no dripping of burning polymer was detected. (Patel et al., 2006)

2.8.2 Carbon Nanotubes (CNTs)

Carbon nanotubes (CNTs) consist of carbon atoms arranged in hexagonal shape that had been rolled into tubes. CNTs had been explored mainly due to their unique properties such as good mechanical and electrical properties. Multi-walled carbon nanotubes (MWNT) were realized as functional fillers in plastic composites in applications such as in paints (Makar and Beaudoin, 2003). It also being studied as reinforcing filler in concrete and had verified to inhibit crack propagation through several performance tests (Makar et al., 2005; Raki et al., 2010).

2.8.3 Carbon Black (CB)

Carbon black (CB) is a nano-particulate amorphous form of carbon. It widely used as filler in rubber or as pigments (Katz and Mileski, 1987). In additions, CB was also used as filler in most of the plastic and paints in order to induce the electrical conductivity. It was verified as a UV stabilizer in plastics application refining the weather ability (Wypych, 1995). However, applications for non-rubber related products have a relatively low market value.

2.8.4 Graphene

Graphene was added in paints and could induce electrical conductivity to the final product. Graphene was a single sheet of graphite in the 2-dimensional counterpart. The single planar sheet of carbon atoms tightly arranged and packed in a hexagonal honeycomb lattice (Geim and Novoselov, 2007). It can also work as filler for conductive and reinforcing applications. The small amount of graphene incorporated as filler to polymer can greatly improve and enhanced the properties such as better mechanical and higher thermal properties (Lu et al., 2013; Zhu et al., 2010).

2.9 Modification of Nanofillers

2.9.1 Modification of Mechanical Properties of Thermoset Composites

Nanoclay was widely used in the application of resin concrete. According to Jo et al. (2008), the pure and modified montmorillonite were added to reinforce a material made of 11% polyester resin and 89% of mineral fillers which was mainly the elementary of sand and limestone. The treated montmorillonite showed that there was increased in the tensile strength and young modulus. The results showed increment of 20% in mechanical properties was achieved with nanofillers composition of 5 wt% to 7 wt% when compared to the untreated montmorillonite.

2.9.2 Modification of Thermophysical Properties of Composites

Seyhan (2008), used double-wall carbon nanotubes (DWCNT) and multi-wall carbon nanotubes untreated and treated (grafted amine functions) in polyester. The treated nanotubes with composition of 0.5 wt% showed increase in tensile strength which was around 5% to 17%.

2.9.3 Modification of Thermal, Mechanical and Electrical properties of Composites

Fukushima et al. (2003) used graphite nanoplatelet treated by O_2 plasma in an acrylamide/benzene solution. Grafted graphite was produced and incorporated to epoxy matrix with a significant aspect ratio showed increased in both thermal and mechanical properties. Another studied on Li et al. (2005), using expanded graphite treated with UV/ozone treatment under normal conditions. Well dispersion and good filler matrix interactions of exfoliated graphite (EG) with epoxy matrix were achieved after ultrasonication. From the results, it showed enhancement in both mechanical and electrical properties.

2.10 Polymer Nanocomposite

In recent years, the expansion of polymer nanocomposites shows a substantial role in the research and advance of nanomaterials. The properties conveyed by the nanoparticles were mainly being emphasis and research on improving the properties of polymer composites such as electrical conduction, strengthening the barrier properties, strengthening the tensile and impact strength and also improvement of flame retardant behaviour as well as thermal properties are being conducted.

The research for synthesis of poly (methyl methacrylate)/graphite nanosheet (PMMA/$Ce(OH)_3$, Pr_2O_3/NanoG) composite was developed. The high aspect ratio structure of the nanosheets played a significant role for the formation of network conductivity in the PMMA matrix.

According to Mo et al. (2005), the incorporation of graphite nanosheets and inorganic nanoparticles to PMMA had showed a better thermal stability from the thermogravimetric analysis (TGA). Results showed that pure PMMA had thermal weight loss at 155 °C whereas the reinforced composite was at 210 °C. Thermal stability had been proven to increase when compared to pure PMMA. The increased in thermal stability was due to the strong filler matrix interactions. The chain movement of the PMMA molecule was trapped by the inorganic nanoparticles which increased the thermal decomposition as it required more

energy. Therefore, the thermal stability of poly (methyl methacrylate)/graphite nanosheet (PMMA/$Ce(OH)_3$, Pr_2O_3/NanoG) composite increased. The TG curves of PMMA and PMMA/$Ce(OH)_3$, Pr_2O_3/NanoG composites were showed in Figure 2.7.

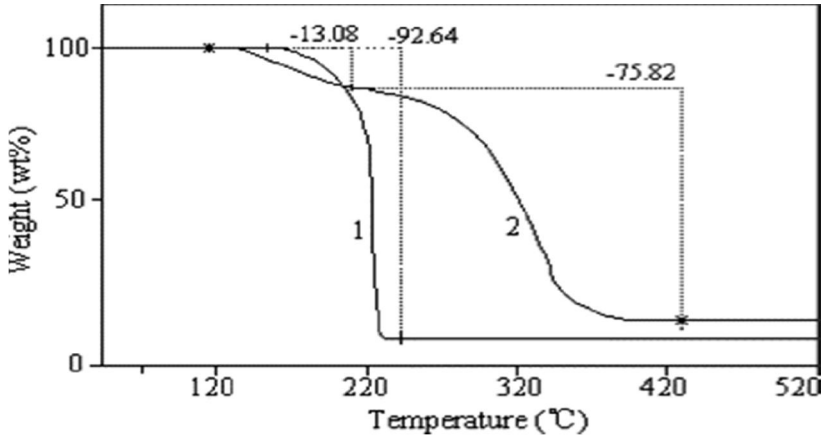

Figure 2.7: TG Curves of (1) PMMA and (2) PMMA/ $Ce(OH)_3$, Pr_2O_3/NanoG Composite (Mo et al., 2005)

CHAPTER 3

METHODOLOGY

3.1 Materials/ Reagents

Graphene oxide (GO) was prepared from the graphite nanofiber (GNF) and other chemicals using the Hummers method. Ultrapure deionized water (DI) was used throughout the process and can be obtained in lab.

The materials and reagents used were as following: Graphite nanofiber (GNF) was supplied by Platinum Senawang Sdn Bhd. Sulphuric acid (H_2SO_4, 95%), Hydrochloric acid (HCl, 37%) and Hydrogen peroxide (H_2O_2, 30%) were obtained from R & M Chemicals. Sodium nitrate ($NaNO_3$) and Potassium permanganate ($KMnO_4$) were purchased from Bendosen Laboratory Chemicals.

3.2 Preparation of Graphite Oxide (GO)

The conventional Hummers method was used for the synthesis of graphene oxide (GO) in this experiment. The experimental set up for the preparation of graphene oxide was shown in Figure 3.1.

Initially, graphite nanofiber (GNF) was prepared in amount of 5.0 g and added into a 500 ml beaker loaded with 115 ml of sulphuric acid (H_2SO_4). Then, the beaker was placed under an overhead stirrer to provide homogeneous stirring at 400 rpm. An ice bath was prepared and used to maintain the temperature of beaker and reaction at 0 ˚C. Next, 2.5 g of sodium nitrate ($NaNO_3$) was added into the beaker.

After the $NaNO_3$ dissolved, 15.0 g of potassium permanganate ($KMnO_4$) was added slowly over 30 minutes to counteract overheating of the reaction mixture (<30˚C). Then, a visible green suspension formed almost instantaneously.

Figure 3.1: Experimental Setup for Preparation of Graphene Oxide (GO)

After 10 minutes of stirring, the solution was separated with the ice bath and the mixture temperature was brought up to approximately 35˚C. Subsequently, a purplish vapour was observed and formed as the mixture was heated up. Then, the solution was stirred vigorously at 500 rpm for duration of 3 hours at room temperature (See Figure 3.2).

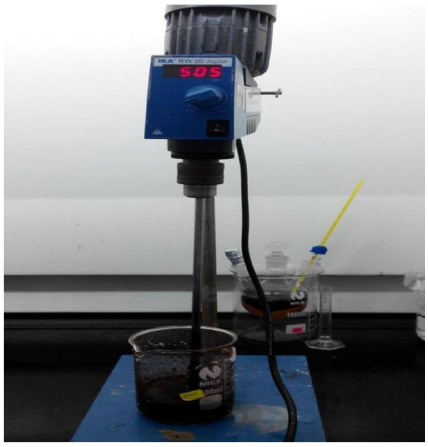

Figure 3.2: Solution Agitated at 500 rpm for 3 hours

After 3 hours, the speed of stirrer was reduced to 400 rpm and a dark brown solution was formed. 230 ml of ultrapure deionized water (DI) was prepared and added slowly into the solution. There was a large exothermic reaction occurred when the water was added. The mixture temperature rose significantly to 70˚C and was maintained until the water was completely added into the solution.

The mixture was then stirred for another 10 minutes and added into 700 ml of ultrapure deionized water. Next, 12 ml of hydrogen peroxide (H_2O_2) was added in order to reduce the residual $KMnO_4$, resulting a light yellow suspension of graphene oxide formed. After that, the mixture was left overnight in the fume hood (See Figure 3.3) and was filtered using the Whatman Anodisc membrane on the next day.

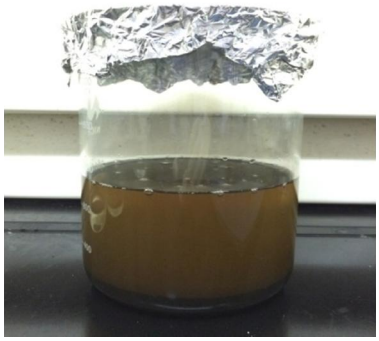

Figure 3.3: GO Solution Left Overnight

Then, the filtered cake obtained was washed with 5 % HCl aliquots solution, followed by deionized water for several times. The washing was carried out using decantation of supernatant with centrifugation with 10,000 rpm for 20 minutes. Finally, the pH value of the supernatant was tested with pH paper and when it reached approximately in between the range of 5 to 7, the product was dispersed in deionized water and dried overnight in an oven at around 80˚C.

3.3 Preparation of Reduced Graphene Oxide (rGO)

The rGO was prepared by chemical reduction of GO. Initially, 0.075 g of GO was added into a 500 ml beaker loaded with 30 ml of ethanol. The GO suspension was then diluted with ultrapure deionized water to 250 ml. Next, the solution was sonicated for 1 hour at room temperature to form well dispersed GO suspension.

After that, 100 ml of formic acid was added into the sonicated solution and the final solution was retained in a three necked round bottom flask. The solution was then stirred for 30 hours for reflux at 100℃ by using a heating mantle with magnetic stirrer. The experimental set up for the preparation of rGO is shown in Figure 3.4.

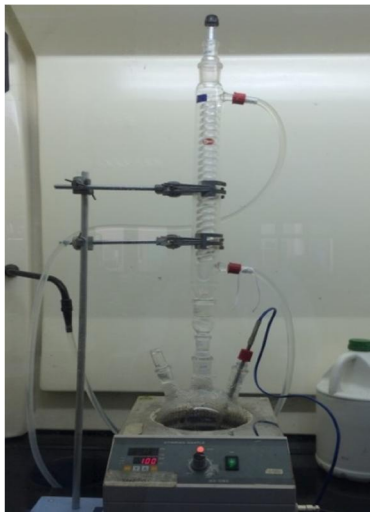

Figure 3.4: Experimental Setup for Preparation of RGO

After 30 hours, the heating mantle was offed. Then, the solution was washed and filtered with methanol, followed by ultrapure deionized water few times until a pure solution formed (see Figure 3.5). Finally, the product was dispersed in deionized water and dried overnight in a vacuum oven at around 80˚C to obtain reduced graphene oxide.

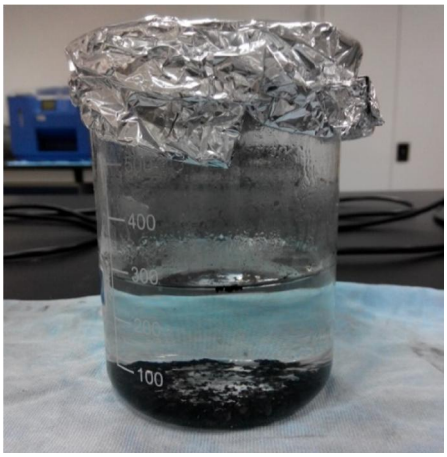

Figure 3.5: Clear Solution Formed After Washed and Filtered

3.4 Characterization of Filler

3.4.1 Fourier Transform Infrared Spectrophotometer (FTIR)

FTIR (Nicolet Photospectrometer 8700) was carried out to provide the information on the chemical bonds and functional group of the reduced graphene oxide (rGO) and high density polyethylene/reduced graphene oxide (HDPE/rGO) nanocomposite. Potassium bromide (KBr) pressed pellet method was applied to test rGO whereas HDPE/rGO nanocomposite was pressed into thin film by hot and cold press and directly used in the FTIR analysis. At first, KBr was added into the specimen and grounded in an agate mortar at a ratio of 1/10 and then the resulting mixture was pressed at 4000 bars for 10 seconds to produce a thin film sample. Analysis was conducted to determine the absorption band between the wavelength ranges of 4000 cm^{-1} to 400 cm^{-1} with 4 scans.

3.4.2 Field Emission Scanning Electron Microscope (FESEM)

FESEM (JOEL JSM 6701F) was used to conduct SEM analysis to determine the plane surface of nanocomposite under magnification of 300X, 500X and 1000X. The samples were cut and stick perpendicularly on a disc with scotch tape. Then, it was coated with a thin layer of platinum. The surface morphology and filler matrix interactions of sample were evaluated using FESEM.

3.4.3 Differential Scanning Calorimetry (DSC)

DSC (Mettler Toledo DSC1/500 Analyzer) was used to conduct analysis to measure the melting point (T_m), recrystallization temperature (T_c) and percentage of crystallinity (X^m_c). The sample was cut into tiny piece and weighted before placed into a 40 μL crucible. Then, the crucible was encapsulated with its lid and ready for characterization. The samples were initially heated from temperature of 0 ˚C to 300 ˚C at a rate of 10˚C/min under nitrogen flow of 15 ml/min and subsequently undergo cooling from 300 ˚C to 0 ˚C.

3.4.4 Melt Flow Index (MFI)

MFI, Tinius Olsen Extrusion Plastometer Model MP600 was used to conduct MFI analysis to determine the flow measurement and viscosity of polymer when molten. The sample was being pushed through a 2mm diameter die and the processing temperature was at 190°C with weight 2.16 kg mass. The data obtained was expressed in grams per 10 minutes (g/10 min).

3.5 Melt Blending of Nanocomposite

Brabender Plastograph EC 815652 Internal Mixer was used to melt and mix the samples at 150 ˚C. The processing torque and time were set to 50 rpm and 10 minutes respectively. The samples were prepared with different rGO loadings as showed in Table 3.1.

3.6 Hydraulic Hot and Cold Press

Hot press, Gotech Hydraulic Hot and Cold Press Machine was used to compress the samples from the internal mixer at 170 ˚C. Preheating time, pressing time and cooling time was fixed to 5 minutes, 2 minutes and 2 minutes respectively.

3.7 Performance Test on Nanocomposite

3.7.1 Impact Testing

The impact testing was conducted using the Izod test under ASTM D256 ISO 180. The load used was 7.5 J. The samples tested were HDPE and HDPE/rGO nanocomposite with different rGO loadings as showed in Table 3.1. All of the testing specimens were prepared in same width, length and thickness which were 12.7 mm, 64 mm and 3.2 mm respectively. Each sample loadings were prepared at least five samples for the impact testing. The testing was run in 5 runs for each sample loadings respectively.

3.7.2 Tensile Testing

Mechanical properties of samples were tested using Universal Testing Machine, WDW-5Y Single Column. The samples tested were HDPE and HDPE/rGO nanocomposite with different composition of rGO as showed in Table 3.1. All the samples were being compressed and cut into dumbbell shaped according to ASTM-D638 standard procedure. The width and thickness of the samples were measured using a digital micrometer. After that, the samples will be tested on the tensile strength, E-modulus and elongation at break at a cross-head speed of 50 mm/min with loading force of 500 N. All results obtained were recorded and the fractured samples were kept for FESEM characterization.

Table 3.1: Different Composition of RGO Distributed

Samples	Weight of HDPE in gram (g)	Weight percentage of rGO (wt%)	Weight of rGO in gram (g)
1	40	0.00	0.00
2	40	0.05	0.02
3	40	0.10	0.04
4	40	0.15	0.06
5	40	0.20	0.08

3.8 Overall Flow Chart of Reduction of Graphene Oxide (GO)

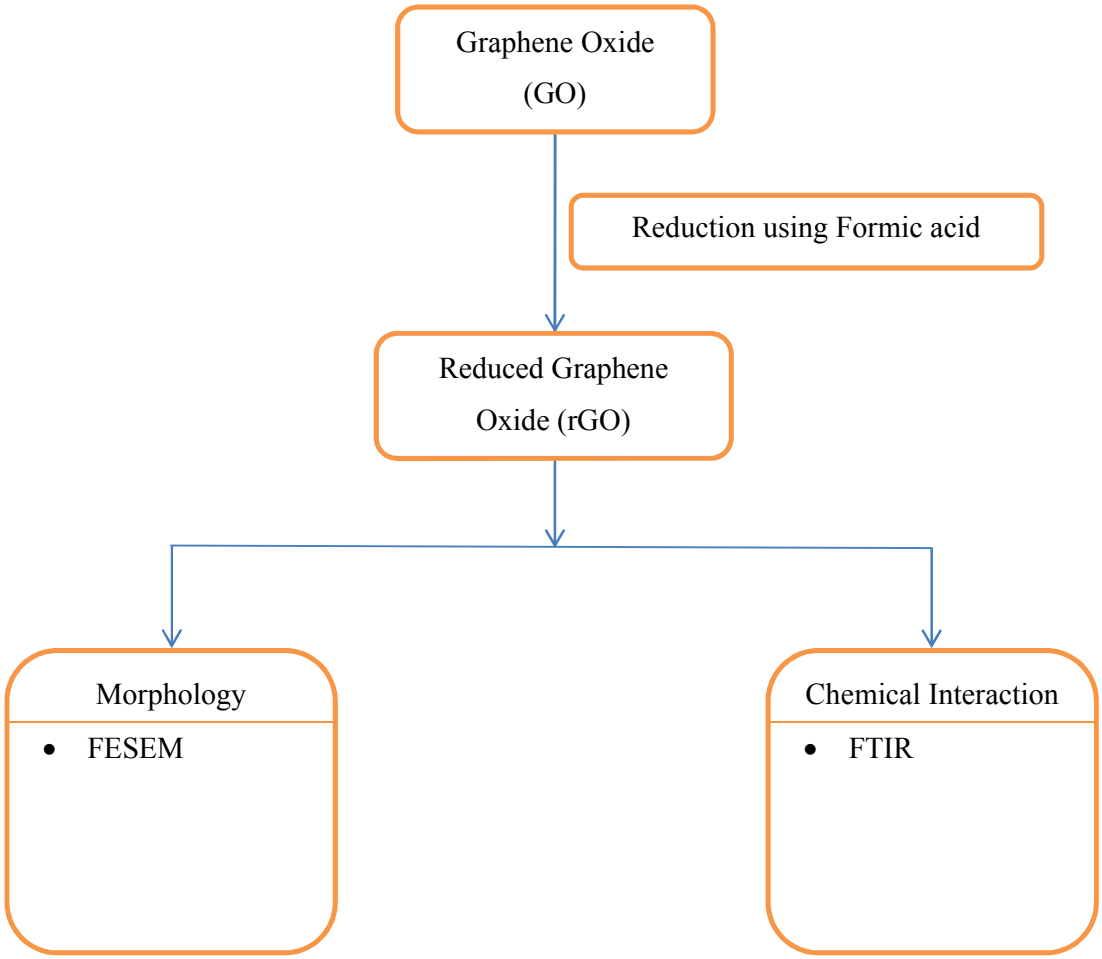

Figure 3.6: Overall Flow Chart of RGO Production

3.9 Overall Flow Chart of Preparation and Characterization of HDPE/rGO Nanocomposite

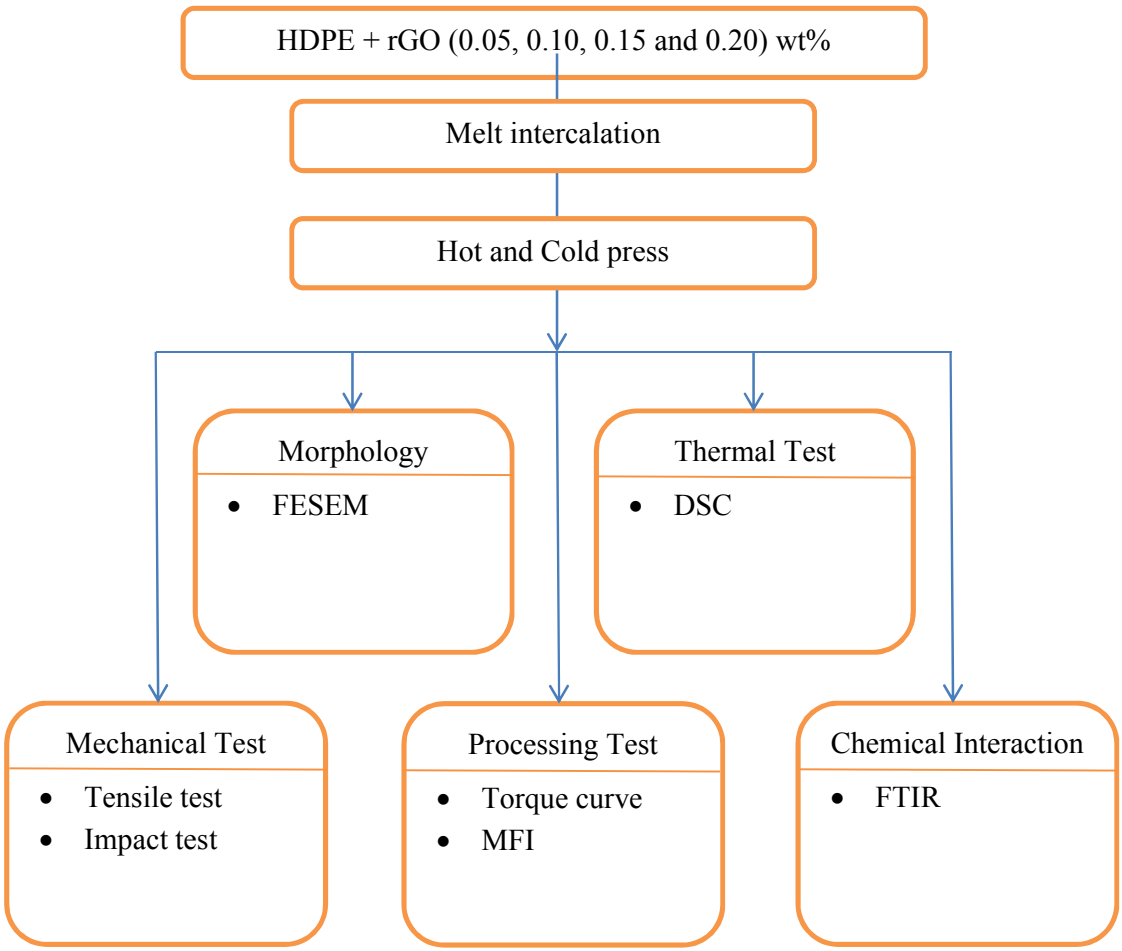

Figure 3.7: Overall Flow Chart of Preparation and Characterization of HDPE/rGO Nanocomposite

CHAPTER 4

RESULTS AND DISCUSSIONS

4.1 Characterization of GO and RGO

4.1.1 Fourier Transform Infrared Spectroscopy (FTIR)

Figure 4.1 showed the IR transmission spectra for both of the GO and rGO. The IR spectra for both GO and rGO were tabulated in Table 4.1.

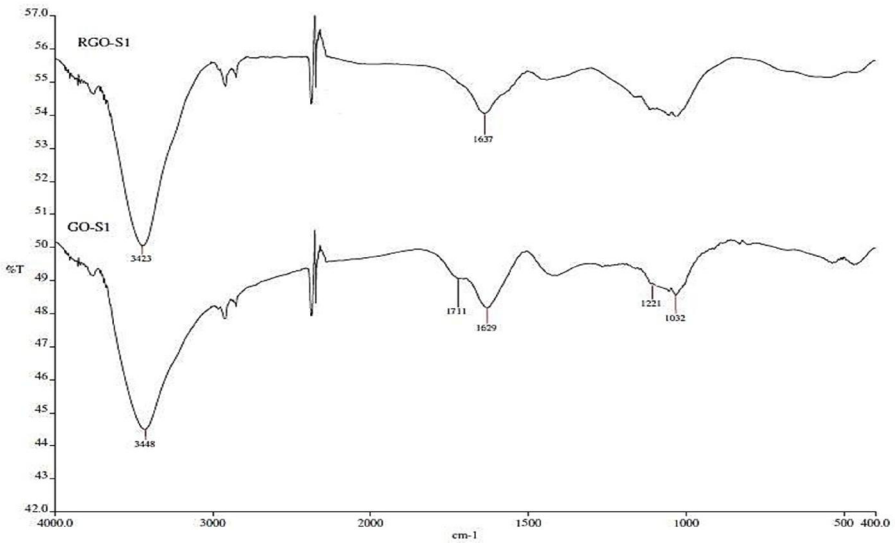

Figure 4.1: IR Spectrum for GO and RGO

Table 4.1: FTIR Spectrum of GO and RGO

Absorption Frequency (cm^{-1})	Absorption Frequency (cm^{-1})		Bond	Functional Groups
	GO	rGO		
3500-3200	3448	3423	O–H Stretch, H-bonded	Alcohols, Phenols, Hydroxyl
1760-1665	1711	-	C=O Stretch	Carbonyls (general)
1640-1585	1629	1637	C=C Stretch	Aromatic C=C bonds
1230-1040	1221	-	C–O–C Stretch	Epoxy
1260-1000	1032	-	C–O Stretch	Alkoxy

IR spectra was conducted to determine the presence of oxygen contained functional groups in GO after the chemical reduction using formic acid. In Table 4.1, GO showed strong and sharp peak around 3448 cm^{-1} which signify the vibration of O–H stretching for hydroxyl group. The peaks at 1711 cm^{-1} and 1629 cm^{-1} signified the vibration of C=O stretching for carbonyl group and aromatic group of C=C bonds respectively. Besides, the peaks at 1221 cm^{-1} and 1032 cm^{-1} were attributed to the vibration of C–O–C stretching of epoxy and C–O stretching of alkoxy respectively.

IR spectra analysis of rGO, peaks at 1711, 1221 and 1032 cm^{-1} obtained in GO was disappeared or partially reduced and the peak at 3448 cm^{-1} was weakened to 3423 cm^{-1}. The peak at 1629 cm^{-1} had slightly increased to 1637 cm^{-1} for the vibration stretching of aromatic C=C bonds. All the peaks were greatly reduced in intensity which indicated that most of the oxygen contained functional groups were successfully removed from GO after the chemical reduction with formic acid. In other words, it means that the GO was successfully reduced to rGO by using formic acid as the reducing agent.

4.1.2 Field Emission Scanning Electron Microscope (FESEM)

FESEM (JOEL JSM 6701F) was used to conduct SEM analysis to determine the surface morphology of GO and rGO. It was observed that the GO exhibits a hair like fiber structure when compared to rGO with flake like structure. The surface morphology of GO obtained was rougher than the rGO. This was due to the presence of oxygen contained functional group which distorted the surface layer. The SEM images for the GO was showed in Figure 4.2 (a) Graphene oxide (GO) and (b) reduced Graphene oxide (rGO).

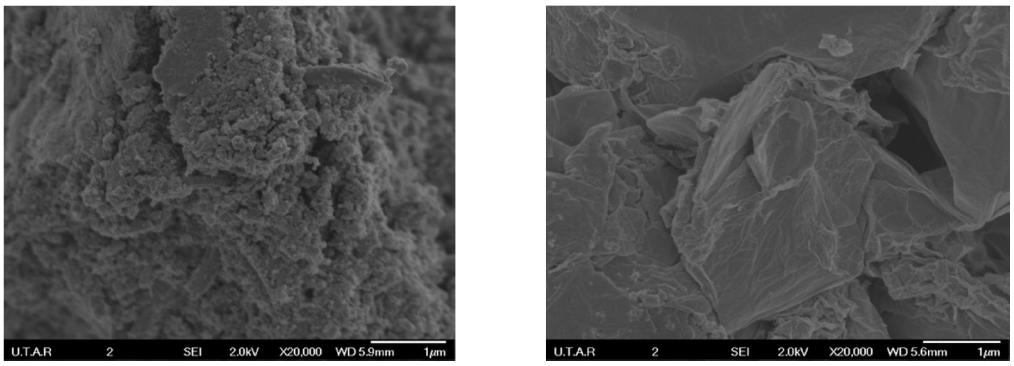

(a) **(b)**

Figure 4.2: SEM Images for (a) Graphene Oxide (GO) and (b) Reduced Graphene Oxide (rGO)

4.2 Processing Properties of HDPE and HDPE/rGO Nanocomposite

4.2.1 Torque Curve

Brabender Plastograph EC 815652 Internal Mixer was used for melt blending to obtain a higher degree of blending and mixing of polymeric materials and their composites in order to achieve optimum properties through homogenous mixing. The mixing of HDPE composite was conducted by using different composition of rGO nanofiller powder to be mixed and determine the torque value obtained. The processing torque and mixing time were set to 50 rpm and 10 minutes respectively, at processing temperature of 150 ˚C. The torque values

obtained for pure HDPE and HDPE/rGO nanocomposite were tabulated in Table 4.2. Figure 4.3 showed the trend of torque values with different rGO loading incorporated to HDPE.

Table 4.2: Torque Values with Different RGO Composition (wt%)

Composite	rGO composition in weight percentage (wt%)	rGO composition in mass (g)	Torque (Nm)
HDPE	0	0	102.0
HDPE/rGO-S1	0.05	0.02	87.1
HDPE/rGO-S2	0.10	0.04	85.8
HDPE/rGO-S3	0.15	0.06	89.7
HDPE/rGO-S4	0.20	0.08	85.4

Based on Figure 4.3, analysis and comparison were done to understand the effect of different composition of rGO nanofiller in HDPE processing torque.

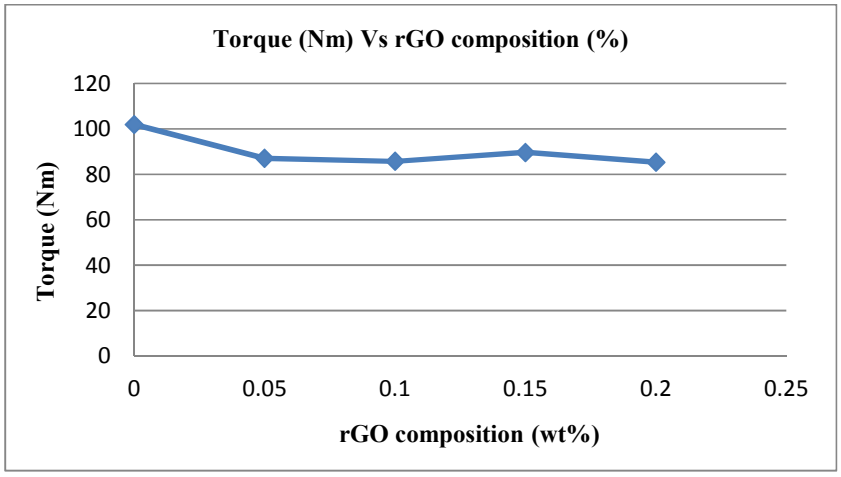

Figure 4.3: Torque (Nm) Against RGO Composition (wt%)

There was slight rise in the torque peak in the 3 minutes. This indicated that the torque value increased due to the solid friction inside the chamber until it was up to one point whereby the solids started to melt. The initial torque value was low as the HDPE was not fully filled inside the mixing chamber at the first few minutes.

Then, the torque value started to increase when the cavity of the chamber was completely filled. The increase in torque with time indicated that there was generation of shear and heat which provide the amount of energy required to melt the HDPE. In additions, it was also the time where rGO nanofiller was started to add into the HDPE compound and being mixed inside the mixer. The stabilization of torque was achieved around 5-9 minutes which indicated that the rGO and HDPE was well mixed. The torque graph results for the pure HDPE and HDPE/rGo nanocomposite can be found in APPENDIX A.

In Table 4.2, the torque values obtained for the pure HDPE and HDPE/rGO nanocomposites were 102.0 Nm, 87.1 Nm, 85.8 Nm, 89.7 Nm and 85.4 Nm respectively. Among all the composite, it was observed that the pure HDPE obtained the highest torque value. When the rGO loading increased in the HDPE composite, there was decrease in torque value as showed in Figure 4.3. The decrement in torque value might due to the addition of rGO nanofiller entered in might stick and remained on the surface of the HDPE which reducing the friction force inside the chamber. Thus, the agitator will required less energy or shear force to rotate the blade as the friction was reduced. Therefore, the torque value will decrease when there was increment in loadings. This also might be the occurrence of agglomerations showed in the SEM images in Figure 4.10 (a), (b) and (d) for different loadings of rGO.

However, in HDPE/rGO-S3 with 0.15 wt% of rGO, the torque value obtained increased which was 89.7 Nm. The increment in the torque value might be due to the addition of rGO lead to increase in total mass of solid and the agitator required more shear force and energy to rotate the blade. At the same time, the rGO added might be well dispersed and well mixed inside the chamber. Thus, the torque is higher when compared to other loadings. This can be supported by the SEM images of HDPE/rGO 0.15 wt% in Figure 4.9 (d) and Figure 4.10 (c), whereby it showed well dispersion of rGO.

4.3 Performance Test for HDPE and HDPE/rGO Nanocomposite

4.3.1 Impact Testing

Figure 4.4 showed the trend of impact values with different rGO loading incorporated to HDPE.

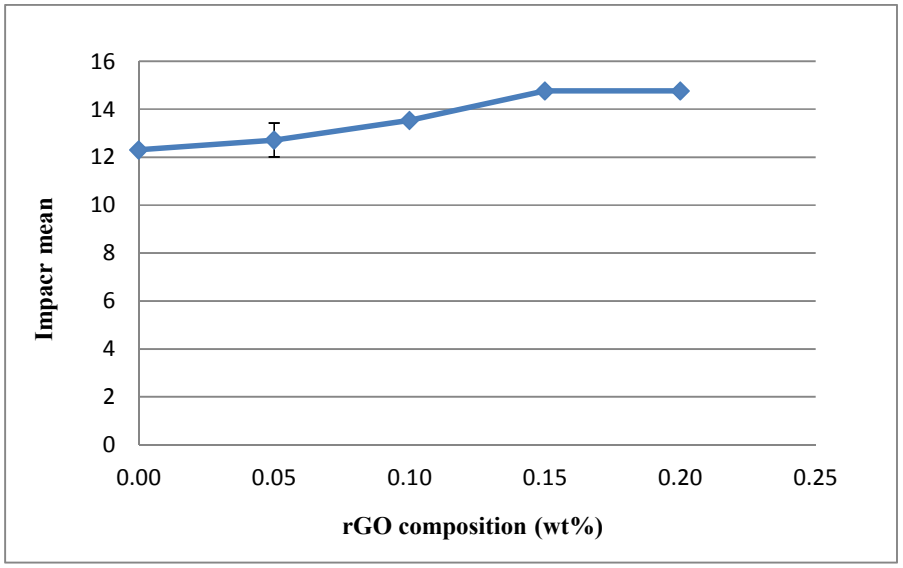

Figure 4.4: Impact (kJ/m^2) Against Different RGO Composition (wt%)

The impact strength of the HDPE/rGO obtained increased with the increment in rGO loadings. The increment in impact strength might due to the addition of rGO which contributed to the increased in the hardness of the HDPE and good filler matrix interfacial interaction between the rGO and HDPE. The rGO structure after incorporated to HDPE allowed it to have free movement and large energy absorption under external loading force (Song et al., 2014).

4.3.2 Tensile Testing

The samples tested were HDPE and HDPE/rGO nanocomposite with different rGO loadings as showed in Table 4.3. All the samples were being compressed and cut into dumbbell shaped according to ASTM-D638 standard procedure. Each sample was prepared at least five samples for the tensile testing. It was tested on the tensile strength, E-modulus and elongation at break at a cross-head speed of 50 mm/min with loading force of 500 N. The graph of E-modulus, tensile strength and elongation at break against the different rGO composition were showed in Figure 4.5 (a), (b) and (c) respectively.

Table 4.3 Tensile Properties of Different HDPE/rGO Nanocomposite

Composite	Composition (wt%)	E-modulus (MPa)	Tensile strength (MPa)	Elongation at break (%)
Pure HDPE	0.00	871	40.63	815.00
HDPE/rGO-S1	0.05	823	32.65	318.87
HDPE/rGO-S2	0.10	824	31.77	151.78
HDPE/rGO-S3	0.15	867	32.95	64.95
HDPE/rGO-S4	0.20	857	32.22	93.21

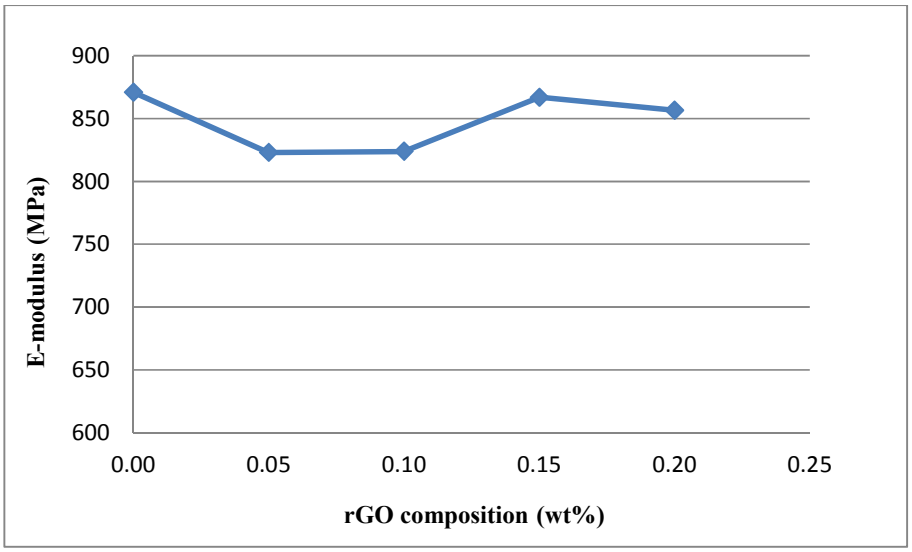

Figure 4.5 (a): E-Modulus (MPa) Against RGO Composition (wt%)

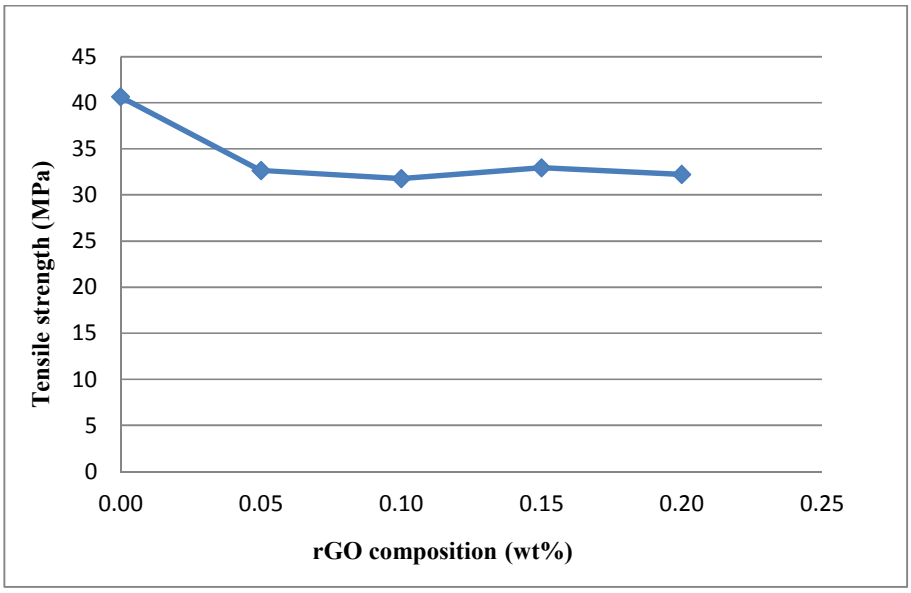

Figure 4.5 (b): Tensile Strength (MPa) Against RGO Composition (wt%)

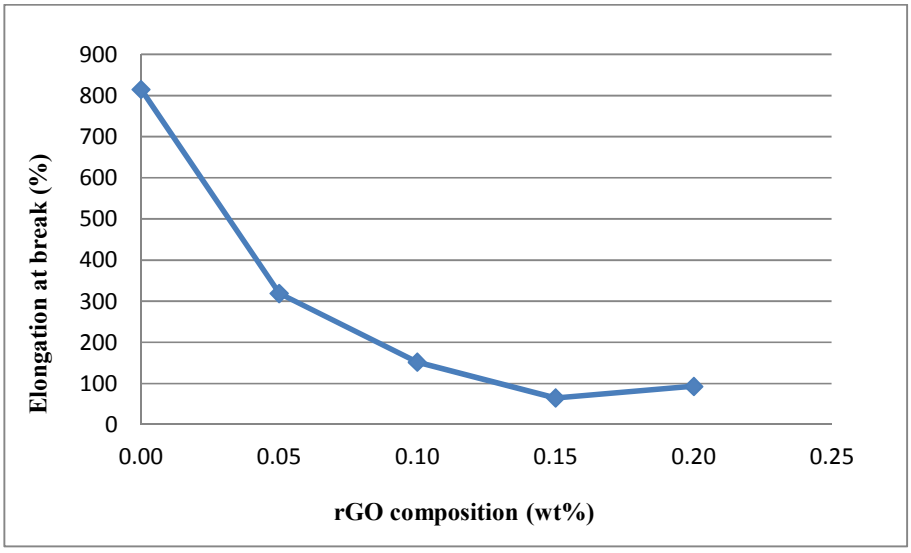

Figure 4.5 (c): Elongation At Break (%) Against RGO Composition (wt%)

From Table 4.3, the E-modulus and tensile strength of the HDPE/rGO nanocomposite gradually decreased in S1 and S2 when compared to pure HDPE. However, it increased in S3 but slightly decreased in S4 for the HDPE/rGO nanocomposite. The E-modulus was defined as the ratio of stress to strain which determine the stiffness of a composite whereas the tensile strength was defined as the maximum loading stress that a composite can withstand before it

breaks. The decreased in e-modulus might be due to the poor interfacial interactions between rGO and HDPE matrix. The interaction of filler with the polymer chain might fail to restrict the chain movement and thus reduced in e-modulus and lead to reduce in tensile strength as well.

For the increment of e-modulus and tensile strength in HDPE/rGO-S3, it might be due to good interfacial interactions between rGO and HDPE matrix. This will enabled the load applied to be transferred through the interactions and contributed to increase in tensile strength. Thus, it can be concluded that the optimum rGO loading incorporated to HDPE was 0.15 wt% which showed increased in e-modulus and tensile strength. The SEM images in Figure 4.9 (d) and Figure 4.10 (c) showed well dispersion of rGO and good filler matrix interaction.

Besides, the SEM images in Figure 4.9 (a), (b), (c), (d) and (e) for the fractured nanocomposites were studied and the results showed that when there was increasing in the rGO loadings, the surface morphology of the nanocomposite became rougher. In additions, agglomeration was observed in the SEM images in Figure 4.10 (a), (b) and (d) whereby the agglomeration formed will act as the stress concentration point in the nanocomposite. The load applied to be transfer through the interactions will become less efficient and contributed to reduce in tensile strength (Igwe and Onuegbu, 2012). This can be supported by the SEM images in Figure 4.10 (a), (b) and (d) which showed microcrack of nanocomposite was formed when force was being applied. Besides, the FTIR results in Figure 4.6 (b) and (c) also showed that there was presence of vibration of C=O stretching for carbonyl groups in the HDPE/rGO nanocomposite which might cause degradation to happen and lead to decrease in tensile strength as well.

For the elongation at break, the results obtained showed that it decreased as the loadings of rGO added increased. Elongation at break was defined as the measurement of a composite ductility. The decreased in elongation at break indicated that the brittleness of HDPE/rGO nanocomposite increased. The decrement in elongation at break might be due to the rGO nanofiller incorporated restricted and demobilised the chain movement of HDPE and lead to the matrix of HDPE become stiffer and decrease in ductility at the same time. This will cause the decrement in elongation at break of the nanocomposite due to the reduced in rigidness and resilience properties of the nanocomposite.

4.4 Characterization of HDPE and HDPE/rGO Nanocomposites

4.4.1 Fourier Transform Infrared Spectroscopy (FTIR)

FTIR spectra analysis for HDPE and HDPE/rGO nanocomposite was conducted using Nicolet Photospectrometer 8700 machine. The samples were prepared through Gotech Hydraulic Hot and Cold Press Machine by pressing it to form into thin film which can be directly used for the IR analysis in the machine without the use of KBr technique. The IR spectra analysis was conducted to examine the effect rGO incorporation to HDPE. Figure 4.6 (a), (b) and (c) showed the IR transmission spectra for different composition of rGO incorporated to HDPE which was 0 wt% (pure), 0.05 wt% and 0.20 wt% respectively. Figure 4.7 showed the IR transmission spectra for rGO together with the pure HDPE and different composition of rGO.

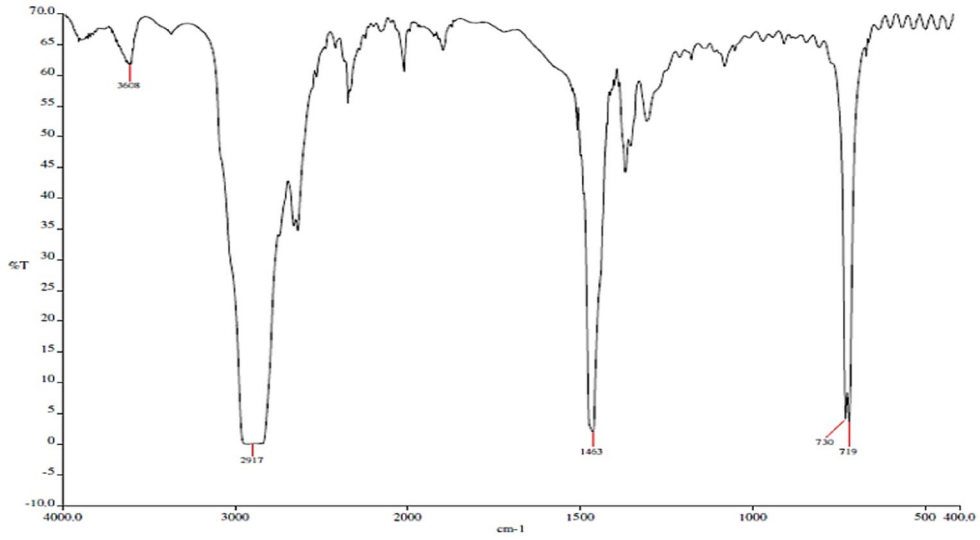

(a) Pure HDPE (0 wt%)

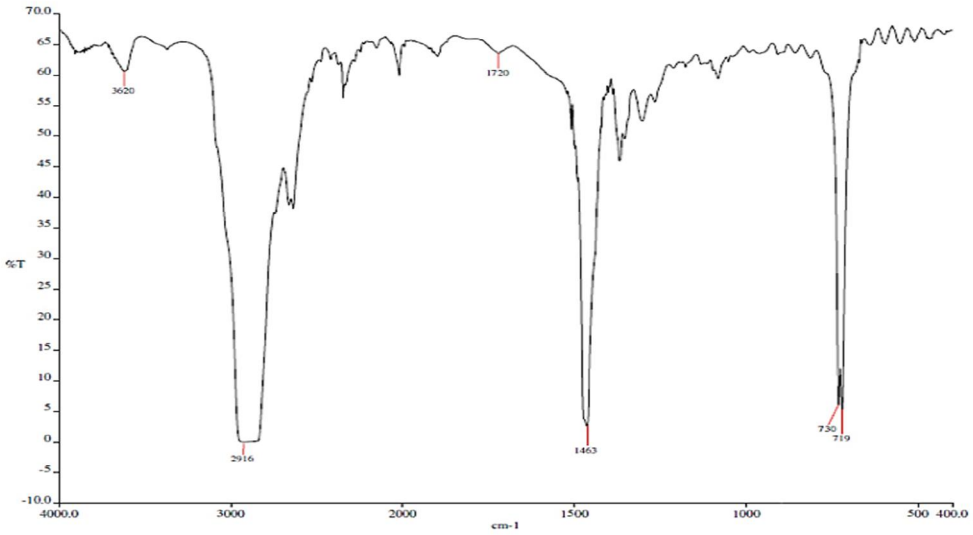

(b) HDPE/rGO 0.05 wt%

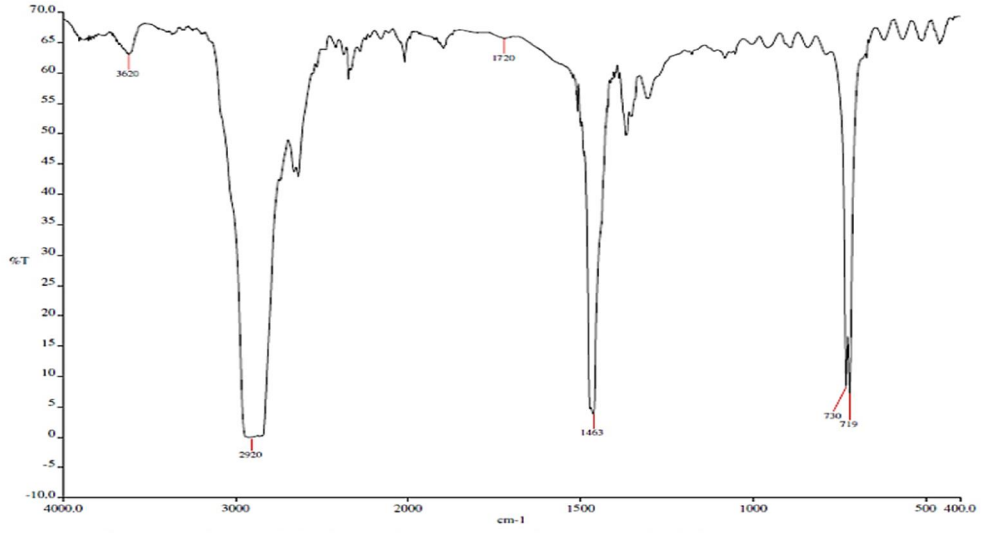

(c) HDPE/rGO 0.20 wt%

Figure 4.6: IR Transmission Spectra of (a) Pure HDPE, (b) HDPE/rGO 0.05 wt% and (c) HDPE/rGO 0.20 wt%

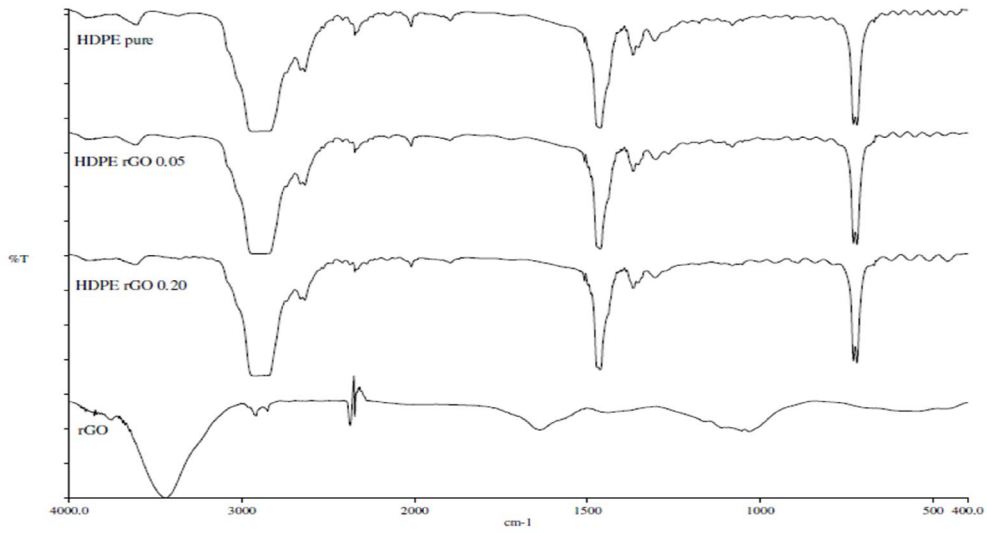

Figure 4.7: IR Spectra of RGO, Pure HDPE and Different Composition of HDPE/rGO Nanocomposite

According to Erbetta et al. (2014) and Krimm et al. (1956), IR spectrums of HDPE consist of four strong peaks which were 2917, 1463, 730 and 719 cm^{-1}. The peak at 2917 cm^{-1} is the vibration of methylene scissoring CH_2 stretching. From the FTIR, the peaks at 2917 cm^{-1} became slightly sharper to 2920 cm^{-1} which indicated the presence of rGO in. The peak at 1720 cm^{-1} was not observed in the IR spectra of HDPE but was observed after the incorporation of rGO which was the vibration of C=O stretching of carbonyl group.

Besides, the peak at 3608 cm^{-1} also shifted to become 3620 cm^{-1} which was the stretching vibration of O–H. All these peaks indicated that the rGO was present and being incorporated to HDPE. The peaks at 1463, 730 and 719 cm^{-1} were the bending vibration and rocking of CH_2 which also contributed to the crystalline region of HDPE. The overall peaks of HDPE were preserved. The IR spectra of HDPE and HDPE/rGO nanocomposite were tabulated in Table 4.4.

Table 4.4: IR Spectra of HDPE and HDPE/rGO Nanocomposite

Absorption Frequency (cm^{-1})		Functional group
Before	**After**	
3608	3620	O–H stretch
2917	2920, 2916	CH_2 stretch
-	1720	C=O stretch
1463	1463	CH_2 bend
730, 719	730, 719	CH_2 rock

4.4.2 Differential Scanning Calorimetry (DSC)

DSC analysis was done on pure HDPE, HDPE/rGO 0.05 wt% and HDPE/rGO 0.20 wt% nanocomposite. The samples were initially heated from 0 ˚C to 300 ˚C at a rate of 10˚C/min under nitrogen flow of 15 ml/min and subsequently undergo cooling from 300 ˚C to 0 ˚C. The thermal properties for pure HDPE, HDPE/rGO 0.05 wt% and HDPE/rGO 0.20 wt% nanocomposite were showed in Figure 4.8. The melting point (T_m), recrystallization temperature (T_c) and crystallinity (X_c^m) were tabulated in Table 4.5. The cystallinity was calculated based on Equation 4.1 (Koldie et al., 2006).

Equation 4.1:

$$X_c^m = \frac{\Delta H_m}{W_p \times \Delta H_{100}} \times 100\ \%$$

Where, ΔH_m = Melting heat, J/g

ΔH_{100} = Melting heat for 100% crystalline HDPE, 293.6 J/g

X_c^m = Crystalliny, %

W_p = Weight fraction of polymer in the sample

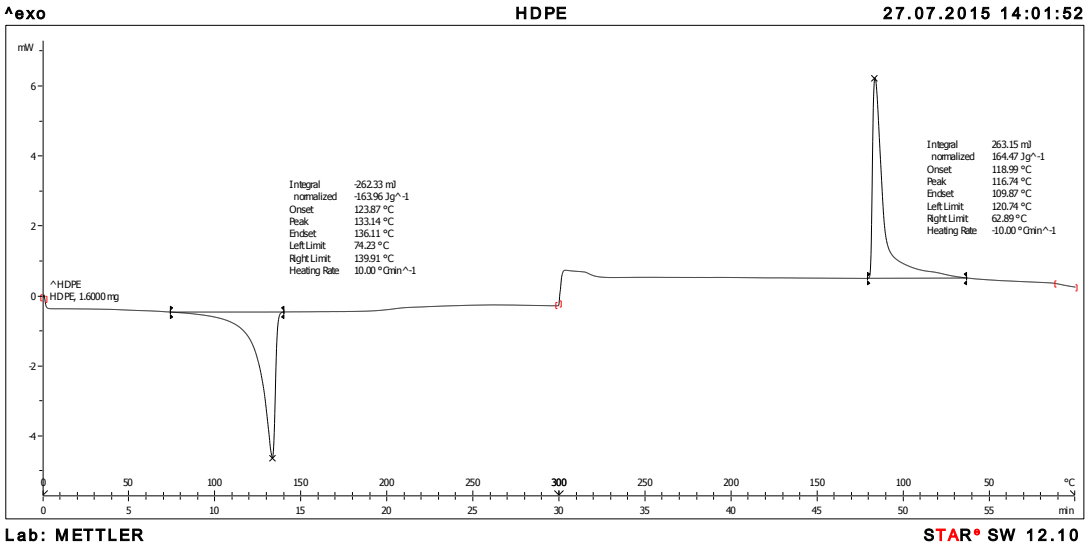

(a) Pure HDPE

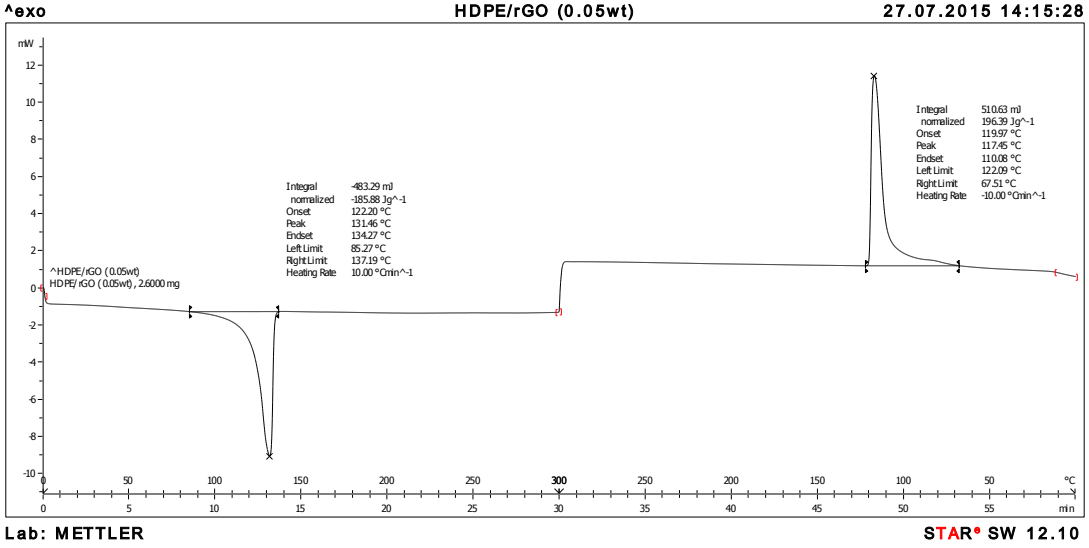

(b) HDPE/rGO 0.05 wt%

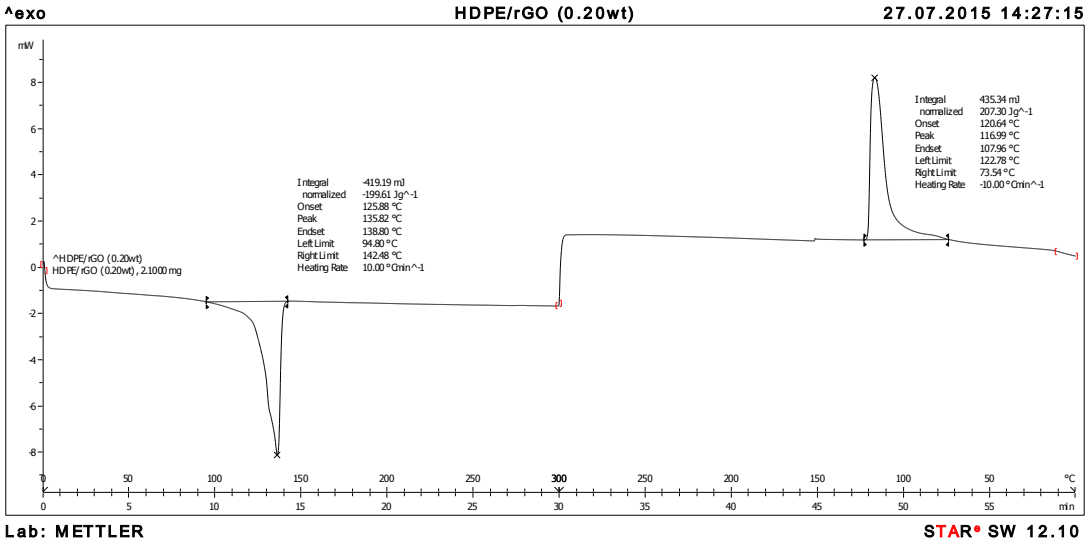

(c) HDPE/rGO 0.20 wt%

Figure 4.8: DSC Results for (a)Pure HDPE, (b) HDPE/rGO 0.05 wt% and (c) HDPE/rGO 0.20 wt%

Table 4.5: DSC Results of Nanocomposite

Composite	Melting temperature, T_m (˚C)	Weight fraction, W_p	ΔH_m (J/g)	Recrystallization temperature, T_c (˚C)	Crystallinity, X^m_c (%)
Pure HDPE	133.14	1.0000	163.96	116.74	55.84
HDPE/rGO 0.05 wt%	131.46	0.9995	185.88	117.45	63.34
HDPE/rGO 0.20 wt%	135.82	0.9980	199.61	116.99	68.12

From the DSC results, it showed that the pure HDPE had an endothermic peak melting temperature of 133.14 ˚C, recrystallization temperature of 116.74 ˚C and crystallinity level of 55.84%. When the rGO loadings increased, the level of crystallinity increased from 55.84% to 68.12%. This might be the rGO affected the HDPE matrix by acting as crystallization nucleus for HDPE (Morimune et al., 2012).

For HDPE/rGO 0.05 wt%, it showed a slightly reduced in melting temperature and increased in recrystallization temperature which was 131.46 ˚C and 117.45 ˚C respectively. The decrease in melting temperature might be due to the presence of rGO disrupted part of the chain formation of crystalline structure. Besides, it might be due to the breakdown of HDPE chain and molecular weight reduction (Colom et al., 2003). However, the melting temperature and recrystallization temperature increased in HDPE/rGO 0.20 wt% which was 135.82 ˚C and 116.99 ˚C respectively. This might be due to the increased in level of crystallinity which eventually lead to increment in melting temperature and recrystallization temperature. This indicated that the thermal stability increased when there was increased in the rGO loadings.

4.4.3 Melt Flow Index (MFI)

The data obtained from MFI was expressed in grams per 10 minutes (g/10 min) and was tabulated in Table 4.6.

Table 4.6: MFI Values of Pure HDPE and HDPE/rGO Nanocomposites

Composite	MFI (g/10min)
Pure HDPE	0.380
HDPE/rGO 0.05 wt%	0.496
HDPE/rGO 0.10 wt%	0.490
HDPE/rGO 0.15 wt%	0.540
HDPE/rGO 0.20 wt%	0.553

From Figure 4.6, the value of MFI obtained increased when higher rGO loadings was introduced to HDPE. This indicated that the viscosity of the nanocomposite decreased as it flow faster with increased in nanofiller loadings. The decreased in flow viscosity might be due to the interaction between the rGO nanofiller and HDPE matrix whereby the chain movement of HDPE was not restricted or free to move (Song et al., 2014). The change in viscosity was depending on the change in the polymer entanglement (Erbetta et al., 2014;

Peacock, 2000). The was no segmental motion of the HDPE/rGO nanocomposite whereby it can flow easily and thus less energy was required to overcome the interactions and a higher MFI value was obtained.

4.4.4 Field Emission Scanning Electron Microscope (FESEM)

FESEM (JOEL JSM 6701F) was used to conduct SEM analysis to determine the plane surface of HDPE and HDPE/rGO nanocomposite under magnification of 300X, 500X and 1000X. Study was done on the surface morphology and interaction between matrix and filler of pure HDPE and HDPE/rGO nanocomposite. The application of the scanning electron microscope (SEM) provided the observation of the surface morphology of the pure HDPE and HDPE/rGO nanocomposite. The surface morphology of pure HDPE and different composition of HDPE/rGO nanocomposites was showed in Figure 4.9 (a), (b), (c), (d) and (e).

For Figure 4.9 (a), the SEM image of pure HDPE showed smooth surface morphology and no matrix tearing. In Figure 4.9 (b), it observed that the HDPE/rGO with 0.05wt% also had a smooth surface morphology with not much difference when compared to pure HDPE. Generally, the smoother the surface morphology of a nanocomposite, it will obtain higher E-modulus and lower elongation at break which eventually lead to increase in stiffness. However, the tensile strength of HDPE/rGO 0.05 wt% decreased which might due to too less filler added which contributed to poor filler matrix dispersion and occurrence of agglomeration as shown in Figure 4.10 (a). The rGO incorporated to HDPE might be too less and as result the filler cannot be dispersed well.

When there was increased in the composition of rGO incorporated to HDPE which was 0.10wt%, 0.15wt% and 0.20wt%, the SEM images observed the surface morphology of nanocomposite become rougher compared to lesser filler loadings. The rougher surface morphology will reduced the E-modulus of nanocomposite. The tensile strength dropped might be due to the poor interfacial interaction between rGO filler and HDPE matrix or agglomeration in certain part. Besides, it also might be the poor filler dispersion whereby the rGO was not distributed uniformly in the HDPE composite (Shibata et al., 2002).

In Figure 4.10 (a), (b) and (d), the SEM image showed that there were formation of agglomeration occurred in different composition of HDPE/rGO nanocomposite. The occurrence of agglomeration of rGO will lead to reduction in tensile strength and E-modulus of the HDPE/rGO nanocomposite.

For HDPE/rGO nanocomposite with 0.15 wt%, the SEM images showed in Figure 4.9 (d) and 4.10 (c), it was observed that there were no agglomerations happened in the structure. This might indicated that there was good dispersion of filler in the matrix. The good dispersion of rGO with the HDPE matrix contributed to increase in tensile strength due to better matrix filler interaction when compared with other filler loadings.

When the rGO loadings increase to 0.20 wt%, the tensile strength was slightly dropped. This might happen due to the high filler loadings added which will increase the difficulties for homogenous dispersion (Supri and Ismail, 2011). Besides, microcrack was observed at 1000X magnification as showed in Figure 4.10 (a), (b) and (d) which lead to reduce in tensile strength as well. The occurrence of microcrack in the structure might due to poor dispersion and interfacial interaction of matrix and filler as well as agglomeration of filler happened. There might be less efficient stress transfer between the two phases of material which was rGO and HDPE (Shibata et al., 2002).

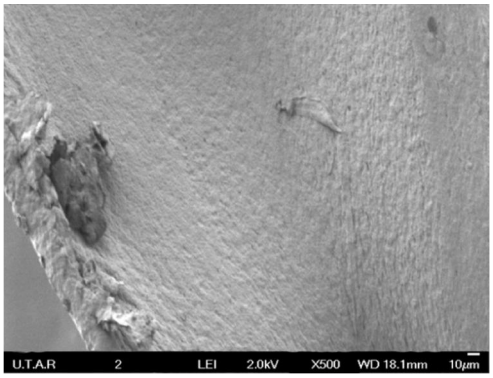

(a) Pure HDPE

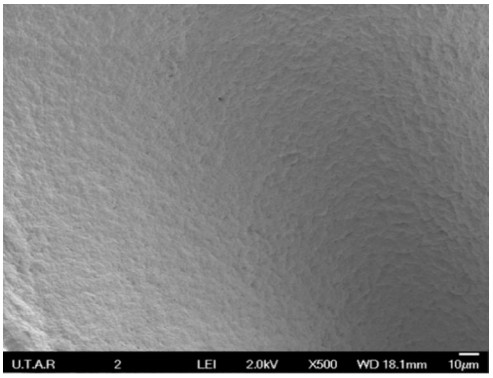

(b) HDPE/rGO 0.05 wt%

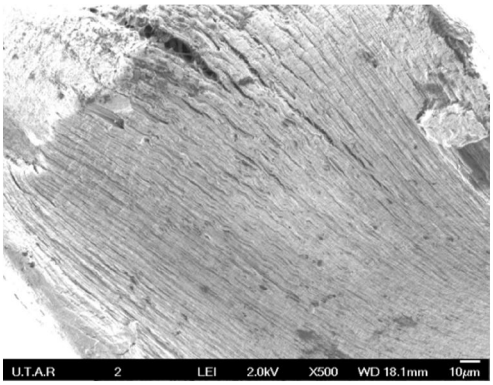

(c) HDPE/rGO 0.10 wt%

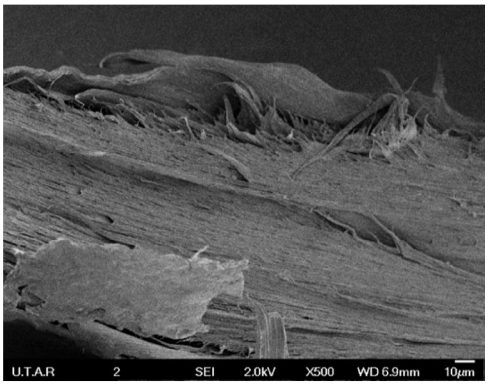

(d) HDPE/rGO 0.15 wt%

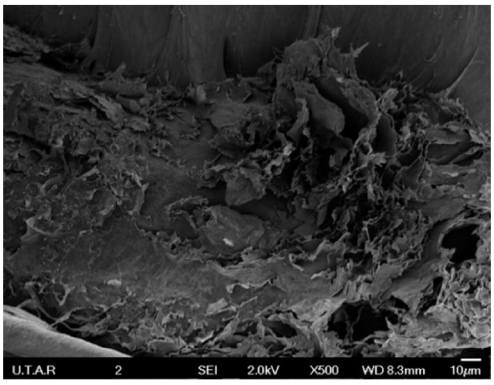

(e) HDPE/rGO 0.20 wt%

Figure 4.9: SEM Images for Surface Morphology of (a) HDPE, (b) HDPE/rGO 0.05 wt%, (c) HDPE/rGO 0.10 wt%, (d) HDPE/rGO 0.15 wt% and (e) HDPE/rGO 0.20 wt%

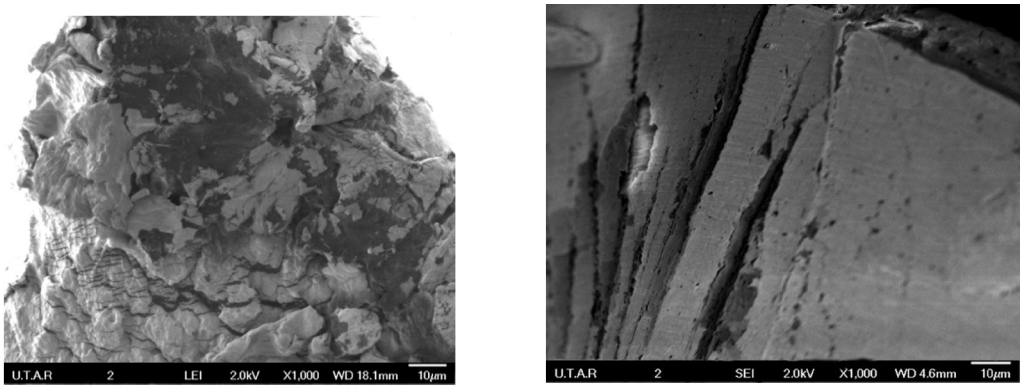

(a) HDPE/rGO 0.05 wt%

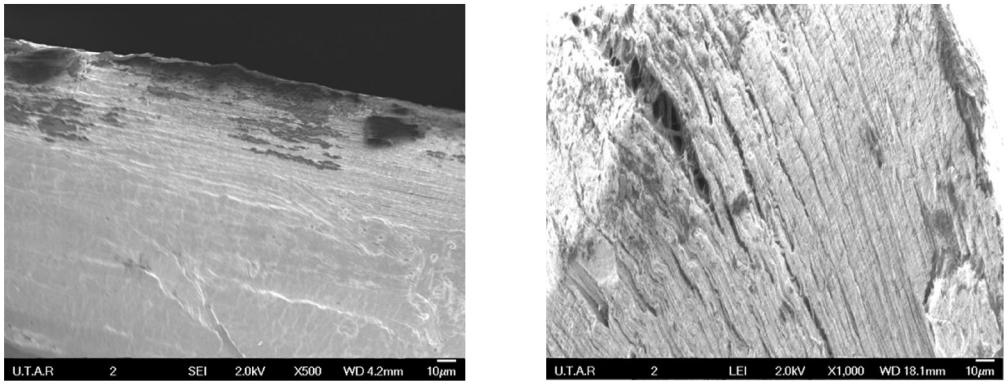

(b) HDPE/rGO 0.10 wt%

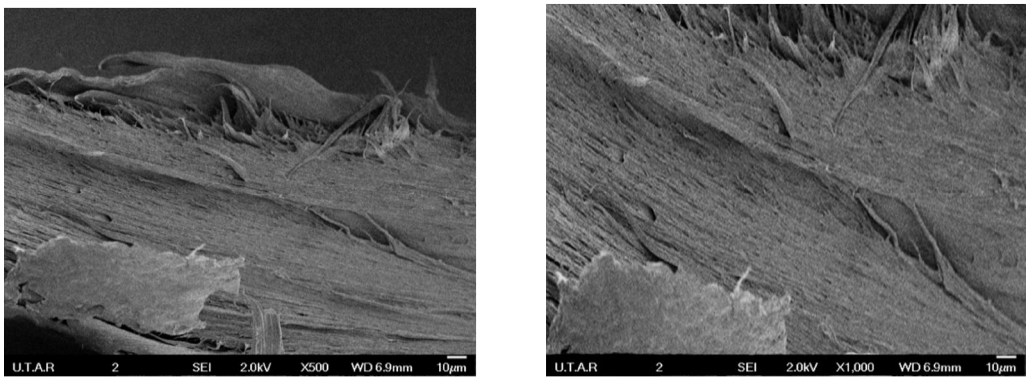

(c) HDPE/rGO 0.15 wt%

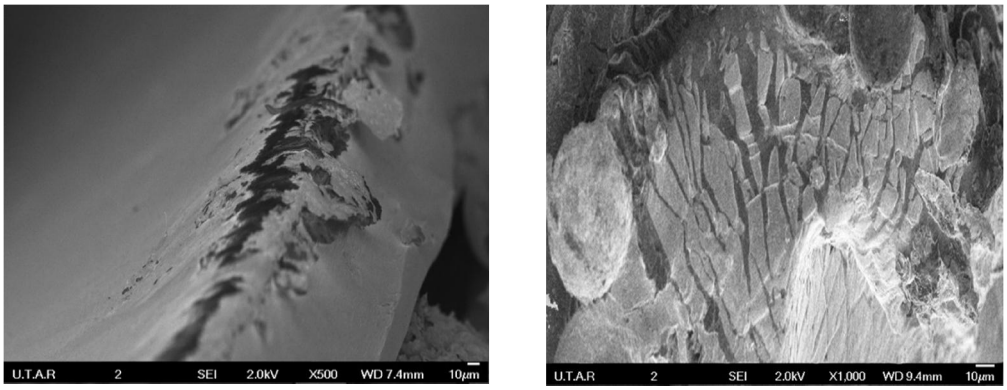

(d) HDPE/rGO 0.20 wt%

Figure 4.10: SEM Images for Agglomeration and Microcrack Observed on (a) HDPE/rGO 0.05 wt%, (b) HDPE/rGO 0.10 wt%, (c) HDPE/rGO 0.15 wt% and (d) HDPE/rGO 0.20 wt%

CHAPTER 5

CONCLUSION AND RECOMMENDATIONS

5.1 Conclusion

In this project, graphene oxide (GO) was successfully produced from graphite nanofiber (GNF) using the conventional Hummer methods. The synthesized GO was then further reduced to reduced graphene oxide (rGO) using the chemical reduction by formic acid.

Characterization test such as FTIR was carried out on both GO and rGO for confirmation on successful oxidation of GNF to GO and reduction of GO to rGO. FTIR results indicated that most of the oxygen contained functional group was removed after the reduction. The rGO was successfully incorporated to HDPE and formed a new HDPE/rGO nanocomposite through melt blending method by using Brabender Internal Mixer.

Characterization of pure HDPE and HDPE/rGO nanocomposite was carried out to determine the morphology and thermal properties. FTIR of HDPE/rGO nanocomposite proved the presence of rGO being incorporated into HDPE at the detected peaks at 3620 cm^{-1} and 2920 cm^{-1} which were the vibrations of O–H stretching and CH_2 stretching respectively. The overall peaks of HDPE stilled preserved. DSC showed that the level of crystallinity increased from 55.84% to 68.12% when the rGO loadings increased. There was increased in both T_m and T_c when higher loadings were being introduced. This indicated that the thermal stability increased when there was increased in the rGO loadings. The MFI value increased which also indicated that there was decreased in flow viscosity of HDPE/rGO nanocomposite when the rGO loadings added was increased.

Performance test such as impact test and tensile test was carried out to determine the mechanical properties of HDPE/rGO nanocomposite. The impact test showed that there was increased in impact strength of the nanocomposite when higher loadings were added. The tensile test showed that the optimum loadings for rGO incorporated to HDPE was 0.15 wt% which showed increased in both e-modulus and tensile strength and decreased in elongation at break.

FESEM was conducted on HDPE/rGO nanocomposite for investigation on the surface morphology and filler matrix interaction. The surface morphology of HDPE/rGO nanocomposite became rougher compared to pure HDPE when higher loadings of rGO were added. It was found that HDPE/rGO nanocomposite with 0.15 wt% had a good dispersion and interfacial interactions between the filler and marix which contributed to increase in mechanical properties.

5.2 Recommendations

In this research, it had proven that the potential of GO and rGO as a promising filler in the future industries. The HDPE/rGO nanocomposite produced was slightly enhanced in both thermal and mechanical properties. However, there was stilled some improvement can be done in the future studies in order to optimise the process and properties of the nanocomposites.

- The reduction process for producing rGO was stilled time consuming and not very effective in removal of the oxygen contained functional group fully. Thus, further research should be done on the process production of rGO in a greener way.

- Studies should be done on the filler size which will influence the filler matrix dispersion and the properties of composite. Current researches had showed that enhancement of properties such as thermal properties can be achieved by a relatively low amount of filler incorporated to the polymer.

REFERENCES

A. Katz, D. (2012). *Graphene*. [online] Available at: http://www.chymist.com/Graphene.pdf [Accessed 23 Mar. 2015].

Allen, M., Tung, V. and Kaner, R. (2010). Honeycomb Carbon: A Review of Graphene. *Chem. Rev.*, 110(1), pp. 132-145.

Azeem, A. (2011). *Polyethylene Maufacturing and its Properties*. *Academia.edu*. [online] Available at: https://www.academia.edu/3052708/Polyethylene_Maufacturing_and_its_Properties [Accessed 8 July 2015].

Bpf.co.uk, (2015). *Polyethylene (High Density) HDPE*. [online] Available at: http://www.bpf.co.uk/plastipedia/polymers/HDPE.aspx [Accessed 8 July 2015].

Brownson, D. A., Kampouris, D. K. and Banks, C. E. (2011). An overview of graphene in energy production and storage applications. *Journal of Power Sources*, 196 (11), pp. 4873—4885.

Carrasco, F. Thermochim. Acta, 213, 115 (1993).

Colom, X. J., Cañavate, J., Suñol J., Pagès, P., Saurina, J. and Carrasco, F. (2003). Natural and artificial aging of polypropylene–polyethylene copolymers. *Journal of Applied Polymer Science*. *87(10)*, pp. 1685-1692.

Dreyer, D. R., Park, S., Bielawski, C. W. and Ruoff, R. S. (2010). The chemistry of graphene oxide. *Chemical Society Reviews*, 39 (1), pp. 228—240.

Erbetta, C., Manoel, G., Oliveira, A., Silva, M., Freitas, R., & Sousa, R. (2014). Rheological and Thermal Behavior of High-Density Polyethylene (HDPE) at Different Temperatures. *MSA*, *05*(13), pp. 923-931.

Erbetta, C.D.C., Silva, M.E.S.R., Freitas, R.F.S. and Sousa, R.G. (2013) Evaluation of Thermal, Chemical and RheologicalProperties of High Density Polyethylene (HDPE) Additives with Pro-Degrading Agent, after Processing. *Proceedingsof the* 12*th Brazilian Congress of Polymers*, *Florianópolis*, pp. 1-4.

Essentialchemicalindustry.org, (2014). *Poly(ethene) (Polyethylene)*. [online] Available at: http://www.essentialchemicalindustry.org/polymers/polyethene.html [Accessed 3 Apr. 2015].

Fisher, M., Kolb, J., & Cole, S. (2004). Enhancing future automotive safety with plastics. In *The 20th International Technical Conference on the Enhanced Safety of Vehicles (ESV), Paper*, pp. 07-0451.

Fukushima, H. and Drazal, L.T. (2003). Graphite Nanocomposites: Structural & Electrical Properties, In: Proceedings of the 14th International Conference on Composite Materials (ICCM-14), San Diego, CA

Ganesh, B., Isloor, A. M. and Ismail, A. (2013). Enhanced hydrophilicity and salt rejection study of graphene oxide-polysulfone mixed matrix membrane. *Desalination*, 313 pp. 199—207.

Gao, W. (2012). Graphite Oxide: Structure, Reduction and Applications.

Gao, J., Liu, F., Liu, Y., Ma, N., Wang, Z. and Zhang, X. (2010). Environment-Friendly Method To Produce Graphene That Employs Vitamin C and Amino Acid. *Chem. Mater.*, 22(7), pp. 2213-2218.

Catalysis-ed.org.uk,. (2015). *Infra-red Spectra for ldpe and hdpe*. [online] Available at: http://www.catalysis-ed.org.uk/polyethene/poly_3_popup.htm [Accessed 8 July 2015].

Geim, A. K. & Novoselov, K. S. (2007). The rise of graphene. *Nature materials*, *6*(3), pp. 183-191.

Geim, A. K. (2009). Graphene: Status and Prospects. *Science*, 324(5934), pp. 1530-1534.

Georgakilas, V., Otyepka, M., Bourlinos, A. B., Ch, Ra, V., Kim, N., Kemp, K. C., Hobza, P., Zboril, R. and Kim, K. S. (2012). Functionalization of graphene: covalent and non-covalent approaches, derivatives and applications. *Chemical reviews*, 112 (11), pp. 6156—6214.

Gerstner, E. (2010). Nobel Prize 2010: Andre Geim & Konstantin Novoselov. *Nature Physics*, 6(11), pp. 836-836.

Guimarães, M.J.O.C., Coutinho, F.M.B., Rocha, M.C.G., Bretas, R.E.S. and Farah, M. (2003) Rheology of High DensityPolyethylene Toughened with Elastomeric Polyethylene. *Polímeros*: *Ciência e Tecnologia*, 13, pp. 135-140.

Hummers W.S. and Offeman R.E. (1958). Preparation of Graphitic Oxide. *Journal of the American Chemical Society*, 80(6), pp. 1339-1339.

Jo, B., Park, S. & Kim, D. (2008). Mechanical properties of nano-mmt reinforced polymer composite and polymer concrete., *Construction and building Materials*, 22, pp. 14–20.

Katz, H. S. and Mileski, J. V. (1987). *Handbook of fillers for plastics*. Springer Science & Business Media.

Kodjie, S.L, Li, L., Li, B.,Cai, W., Li, C.Y. and Keating, M., (2006). Morphology and Crystallization Behaviour of HDPE/CNT Nanocomposies. *Journal of Macromolecular Science*, 45, pp. 231-245.

Krimm, S., Liang, C., & Sutherland, G. (1956). Infrared Spectra of High Polymers. II. Polyethylene. *The Journal Of Chemical Physics*, 25(3), pp. 549.

Icis.com,. (2015). *Polyethylene - high density (HDPE) Production and Manufacturing Process*. [online] Available at: http://www.icis.com/resources/news/2007/11/06/9076153/polyethylene-high-density-hdpe-production-and-manufacturing-process/ [Accessed 8 July 2015].

Igwe I.O and Onuegbu G.C. (2011), 'The Effects of Filler Contents and Particle Sizes on the Mechanical and End-Use Properties of Snail Shell Powder Filled Polypropylene. *Mat.Sci.Appl*. 2, pp. 801 - 809.

Lau, K. Y., & Piah, M. A. M. (2011). Polymer nanocomposites in high voltage electrical insulation perspective: a review. *Malaysian Polymer Journal*, *6*(1), pp. 58-69.

Li, J., Kim, J.K. and Sham, M.L. (2005). Conductive Graphite Nanoplatelet/Epoxy Nanocomposites: Effects of Exfoliation and UV/ozone Treatment of Graphite. *Scripta Materialia*, 53, pp. 235–240

Liu, H., Wu, Q., Han, G., Yao, F., Kojima, Y., & Suzuki, S. (2008). Compatibilizing and toughening bamboo flour-filled HDPE composites: Mechanical properties and morphologies. *Composites Part A: Applied Science And Manufacturing*, *39*(12), pp. 1891-1900.

Lu, J., Negulescu, I., & Wu, Q. (2005). Maleated wood-fiber/high-density-polyethylene composites: Coupling mechanisms and interfacial characterization. *Composite Interfaces*, 12(1-2), pp. 125-140.

Lu, Y., Yang, X. and Su, B. (2013). Self-assembly to monolayer graphene film with high electrical conductivity.*Journal of Energy Chemistry*, 22 (1), pp. 52-57.

Makar, J.M. and Beaudoin, J.J. (2003). Proceedings of 1st International Symposium on Nanotechnology in Construction, Paisley, Scotland.

Makar, J.M., Margeson, J., Luh, J. (2005). Carbon nanotube/cement composites-early results and potential applications, *Construction Materials*, pp. 32.

Marcano, D. C., Kosynkin, D. V., Berlin, J. M., Sinitskii, A., Sun, Z., Slesarev, A., Alemany, L. B., Lu, W. and Tour, J. M. (2010). Improved synthesis of graphene oxide. *ACS nano*, 4 (8), pp. 4806-4814.

Mitra, M., Chatterjee, K., Kargupta, K., Ganguly, S. and Banerjee, D. (2013). Reduction of graphene oxide through a green and metal-free approach using formic acid. *Diamond and Related Materials*, 37, pp. 74-79.

Mo, Z., Sun, Y., Chen, H., Zhang, P., Zuo, D., Liu, Y., & Li, H. (2005). Preparation and characterization of a PMMA/Ce(OH)3, Pr2O3/graphite nanosheet composite. *Polymer*, *46*(26), pp. 12670-12676.

Morimune, S., Nishino, T., & Goto, T. (2012). Poly(vinyl alcohol)/graphene oxide nanocomposites prepared by a simple eco-process. *Polym J*, *44*(10), pp. 1056-1063.

Nobelprize.org, (2010), *Graphene* (2010) [online] Available at: http://www.nobelprize.org/nobel_prizes/physics/laureates/2010/advanced-physicsprize2010.pdf [Accessed 23 Mar. 2015].

Park, S., Dikin, D. A., Nguyen, S. T. and Ruoff, R. S. (2009). Graphene oxide sheets chemically cross-linked by polyallylamine. *The Journal of Physical Chemistry C*, 113 (36), pp. 15801—15804.

Patel, H., Somani, R., Bajaj, H., & Jasra, R. (2006). Nanoclays for polymer nanocomposites, paints, inks, greases and cosmetics formulations, drug delivery vehicle and waste water treatment. *Bulletin Of Materials Science*, *29*(2), pp. 133-145.

Peacock, A.J. (2000). Handbook of Polyethylene—Structures, Properties and Applications. CRC Press.

Pei, S. and Cheng, H. (2012). The reduction of graphene oxide. *Carbon*, 50(9), pp. 3210-3228.

Plasmat.com, (2008). *Polyethylene*. [online] Available at: http://www.plasmat.com.tr/information-POLYETHYLENE-14.html [Accessed 25 Feb. 2015].

Prospector.com, (2014). *HDPE :High Density Polyethyelene*. [online] Available at: http://www2.ulprospector.com/pm/HDPE.asp [Accessed 25 Feb. 2015].

Raki, L., Beaudoin, J., Alizadeh, R., Makar, J., & Sato, T. (2010). Cement and Concrete Nanoscience and Nanotechnology. *Materials*, *3*(2), 918-942.

Scifun.org, (2012). *Chemical of the week: Polymers*. [online] Available at: http://scifun.chem.wisc.edu/chemweek/PDF/Polymers.pdf [Accessed 25 Feb. 2015].

Sekhar C.Ray (2015), 'Applications of Graphene and Graphene-Oxide Based Nanomaterials', *A volume in Micro and Nano Technologies*, pp. 1-38

Seyhan, a. (2008). *development of multi and double walled carbon nanotubes (cnts)/ vinylester nanocomposites* (1st ed.). [online] Available at: http://library.iyte.edu.tr/tezler/doktora/makinamuh/T000677.pdf [Accessed 8 July 2015].

Shao, G., Lu, Y., Wu, F., Yang, C., Zeng, F. and Wu, Q. (2012). Graphene oxide: the mechanisms of oxidation and exfoliation. *Journal of Materials Science*, 47 (10), pp. 4400—4409.

Song, J., Yang, W., Fu, F., & Zhang, Y. (2014). The Effect of Graphite on the Water Uptake, Mechanical Properties, Morphology, and EMI Shielding Effectiveness of HDPE/Bamboo flour composites. *Bioresources*, *9*(3).

Shibata, M., Takachiyo, K., Ozawa, K., Yosomiya, R., Takeishi, H. (2002) Biodegradable polyester composites reinforced with short abaca fiber. *J. Appl. Polym. Sci*. 85, pp. 129–138

Spencer, D. (2015). *Case Study: (HDPE) Outdoors Application*. *Madisongroup.com*. [online] Available at: http://www.madisongroup.com/case-studies-outdoor-hdpe.html [Accessed 8 July 2015].

Stankovich, S., Dikin, D.A., Piner, R.D., Kohlhaas, K.A., Kleinhammes, A. (2007). Synthesis of graphene-based nanosheets via chemical reduction of exfoliated graphite oxide. *Carbon*, 45, pp. 1558 – 1565.

Supri, A., Ismail, H., & Shuhadah, S. (2010). Effect of Polyethylene-Grafted Maleic Anhydride (PE- g -MAH) on Properties of Low Density Polyethylene/Eggshell Powder (LDPE/ESP) Composites. *Polymer-Plastics Technology And Engineering*, *49*(4), pp. 347-353.

Szeteiová, K. (2010). Automotive materials plastics in automotive markets today. *Institute of Production Technologies, Machine Technologies and Materials, Faculty of Material Science and Technology in Trnava, Slovak University of Technology Bratislava*.

Tapplastics.com, (2015). *Smooth Polyethylene Sheets - HDPE (Rigid High-Density Polyethylene)*. [online] Available at: http://www.tapplastics.com/product/plastics/cut_to_size_plastic/hdpe_sheets/529 [Accessed 8 July 2015].

Torres, A.A.U. (2007) Physicochemical Ageing of HDPE Pipes Assigned to the Transportation of Petroleum Derivatives.M.Sc. Dissertation, Catholic University of Rio de Janeiro, Rio de Janeiro.

Thongruang, W. (2002). Correlated electrical conductivity and mechanical property analysis of high-density polyethylene filled with graphite and carbon fiber. *Polymer*, 43(8), pp. 2279-2286.

Upcinc.com, (2010). *HDPE :High Density Polyethyelene*. [online] Available at: http://www.upcinc.com/resources/materials/HDPE.html [Accessed 25 Feb. 2015].

Wypych G. (1995). Handbook of Material Weathering, 2nd Edition, ChemTex Publishing, Canada, pp. 328.

Zerbi, G.; Galiano, G.; Fanti, N. D. and Baini, L. Polymer, 30, 2324 (1989).

Zhang, X., Li, K., Li, H., Lu, J., Fu, Q. and Chu, Y. (2014). Graphene nanosheets synthesis via chemical reduction of graphene oxide using sodium acetate trihydrate solution. *Synthetic Metals*, 193, pp. 132-138.

Zhang, X., Li, K., Li, H. and Lu, J. (2013). Dipotassium hydrogen phosphate as reducing agent for the efficient reduction of graphene oxide nanosheets. *Journal of Colloid and Interface Science*, 409, pp. 1-7.

Zhao, L., Guo, Z., Cao, Z., Zhang, T., Fang, Z., & Peng, M. (2013). Thermal and thermo-oxidative degradation of high density polyethylene/fullerene composites. *Polymer Degradation And Stability*, *98*(10), pp. 1953-1962.

Zhu, Y., Murali, S., Cai, W., Li, X., Suk, J. W., Potts, J. R. and Ruoff, R. S. (2010). Graphene and graphene oxide: synthesis, properties, and applications. *Advanced materials*, 22 (35), pp. 3906-3924.

APPENDICES

APPENDIX A : Data Results for Torque Curves

BRABENDER® Plastogram

PLASTI-CORDER and Mixer Measuring Head
Fusion Behaviour / Version 4.2.10

Test Conditions

Order	: HDPE2		Speed	:	50 1/min
Operator	: woh		Mixer Temp.	:	150 °C
Date	: 27/5/2015 09:06		Start Temp.	:	144 °C
Drive Unit	: Plastograph EC		Meas. Range	:	100 Nm
Mixer	: W 50 EHT - 3 Zones		Damping	:	0
Loading Chute	: Manual + 5 kg		Test Time	:	10.00 min
Sample	: HDPE2		Sample Mass	:	40.0 g
Additive	:		Code Number	:	

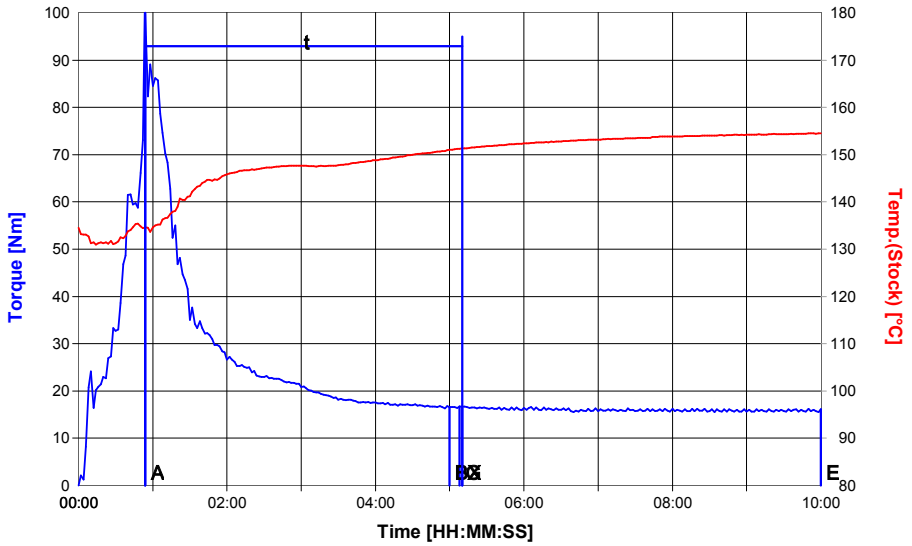

Name		Time [HH:MM:SS]	Torque [Nm]	Stock Temp. [°C]
Loading Peak	A	00:00:54	102.0	135
Minimum	B	00:05:00	16.6	151
Inflection Point	G	00:05:08	16.7	151
Maximum	X	00:05:10	16.7	151
End	E	00:10:00	16.2	155

Integration / Energy

Loading Peak	to Minimum	A - B	16.3	[kNm]
Minimum	to Maximum	B - X	0.4	[kNm]
Maximum	to End	X - E	11.2	[kNm]
Loading Peak	to Maximum	A - X	16.7	[kNm]
Loading Peak	to End (W)	A - E	27.9	[kNm]
Specific Energy(W/Sample Mass)			697.9	[kNm/kg]
Gelation Area above B		B - X	0.0	[kNm]

Results

Fusion Time t	A - X	00:04:16	[HH:MM:SS]
Gelation Speed v		-3.4	[Nm/min]

BRABENDER® Plastogram

PLASTI-CORDER and Mixer Measuring Head
Fusion Behaviour / Version 4.2.10

Test Conditions

Order	: HDPE_0.05rGO2		Speed	:	50 1/min
Operator	: woh		Mixer Temp.	:	150 °C
Date	: 27/5/2015 09:57		Start Temp.	:	147 °C
Drive Unit	: Plastograph EC		Meas. Range	:	100 Nm
Mixer	: W 50 EHT - 3 Zones		Damping	:	0
Loading Chute	: Manual + 5 kg		Test Time	:	10.00 min
Sample	: HDPE_0.05rGO2		Sample Mass	:	40.0 g
Additive	: rGO		Code Number	:	

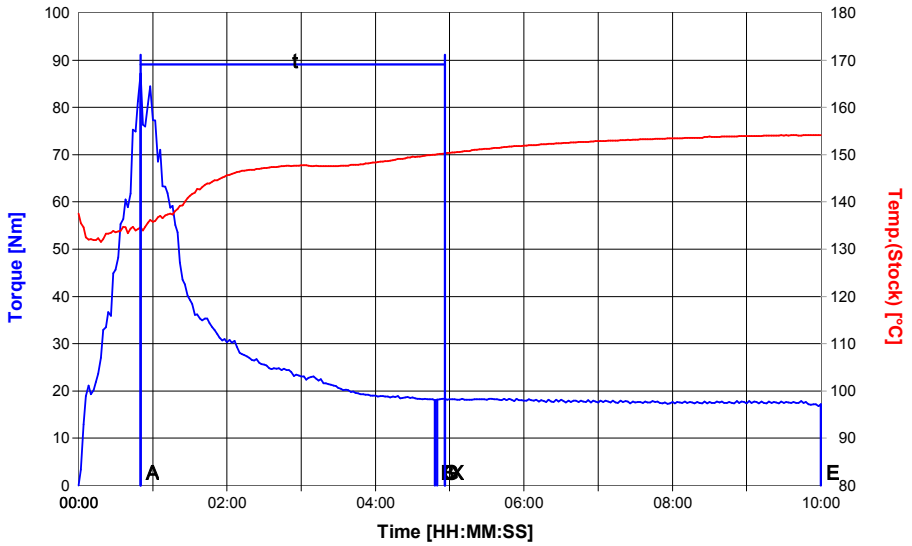

Name		Time [HH:MM:SS]	Torque [Nm]	Stock Temp. [°C]
Loading Peak	A	00:00:50	87.1	135
Minimum	B	00:04:48	18.1	150
Inflection Point	G	00:04:50	18.2	150
Maximum	X	00:04:56	18.3	150
End	E	00:10:00	17.2	154

Integration / Energy

Loading Peak	to Minimum	A - B	17.3	[kNm]
Minimum	to Maximum	B - X	0.4	[kNm]
Maximum	to End	X - E	13.0	[kNm]
Loading Peak	to Maximum	A - X	17.7	[kNm]
Loading Peak	to End (W)	A - E	30.6	[kNm]
Specific Energy(W/Sample Mass)			766.0	[kNm/kg]
Gelation Area above B		B - X	0.0	[kNm]

Results

Fusion Time t	A - X	00:04:06	[HH:MM:SS]
Gelation Speed v		2.9	[Nm/min]

BRABENDER® Plastogram

PLASTI-CORDER and Mixer Measuring Head
Fusion Behaviour / Version 4.2.10

Test Conditions

Order	: HDPErGO0.04	Speed	:	50	1/min
Operator	: woh	Mixer Temp.	:	150	°C
Date	: 15/7/2015 17:06	Start Temp.	:	134	°C
Drive Unit	: Plastograph EC	Meas. Range	:	100	Nm
Mixer	: W 50 EHT - 3 Zones	Damping	:	0	
Loading Chute	: Manual + 5 kg	Test Time	:	10.00	min
Sample	: HDPErGO0.04	Sample Mass	:	40.0	g
Additive	: rgo0.04	Code Number	:		

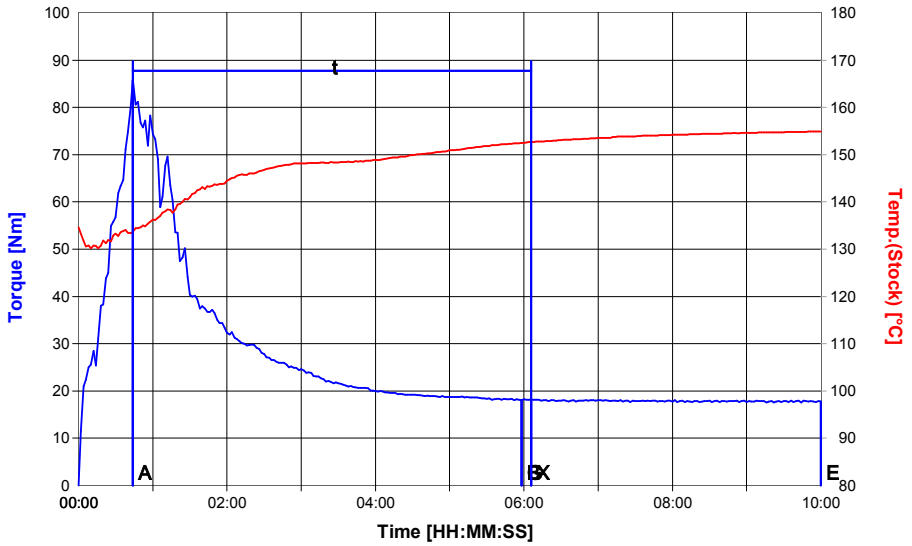

Name		Time [HH:MM:SS]	Torque [Nm]	Stock Temp. [°C]
Loading Peak	A	00:00:44	85.8	134
Minimum	B	00:05:58	18.0	153
Inflection Point	G	00:05:58	18.0	153
Maximum	X	00:06:06	18.2	153
End	E	00:10:00	17.8	155

Integration / Energy

Loading Peak	to Minimum	A - B	21.1	[kNm]
Minimum	to Maximum	B - X	0.5	[kNm]
Maximum	to End	X - E	9.5	[kNm]
Loading Peak	to Maximum	A - X	21.6	[kNm]
Loading Peak	to End (W)	A - E	31.1	[kNm]
Specific Energy(W/Sample Mass)			776.6	[kNm/kg]
Gelation Area above B		B - X	0.2	[kNm]

Results

Fusion Time t	A - X	00:05:22	[HH:MM:SS]
Gelation Speed v		5.7	[Nm/min]

BRABENDER® Plastogram

PLASTI-CORDER and Mixer Measuring Head
Fusion Behaviour / Version 4.2.10

Test Conditions

Order	: HDPErGO0.15wt	Speed	:	50	1/min
Operator	: woh	Mixer Temp.	:	150	°C
Date	: 6/7/2015 16:12	Start Temp.	:	147	°C
Drive Unit	: Plastograph EC	Meas. Range	:	100	Nm
Mixer	: W 50 EHT - 3 Zones	Damping	:	0	
Loading Chute	: Manual + 5 kg	Test Time	:	10.00	min
Sample	: HDPErGO0.15wt	Sample Mass	:	40.0	g
Additive	: rGO0.15wt	Code Number	:		

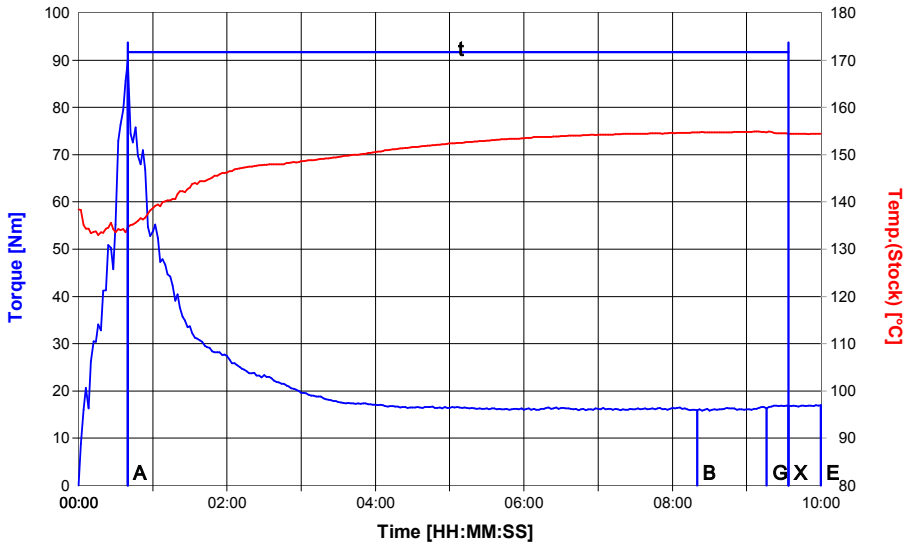

Name		Time [HH:MM:SS]	Torque [Nm]	Stock Temp. [°C]
Loading Peak	A	00:00:40	89.7	135
Minimum	B	00:08:20	15.9	155
Inflection Point	G	00:09:16	16.4	155
Maximum	X	00:09:34	16.9	154
End	E	00:10:00	17.0	154

Integration / Energy

Loading Peak	to Minimum	A - B	23.0	[kNm]
Minimum	to Maximum	B - X	2.7	[kNm]
Maximum	to End	X - E	1.0	[kNm]
Loading Peak	to Maximum	A - X	25.8	[kNm]
Loading Peak	to End (W)	A - E	26.8	[kNm]
Specific Energy(W/Sample Mass)			668.8	[kNm/kg]
Gelation Area above B		B - X	0.1	[kNm]

Results

Fusion Time t	A - X	00:08:54	[HH:MM:SS]
Gelation Speed v		5.5	[Nm/min]

BRABENDER® Plastogram

PLASTI-CORDER and Mixer Measuring Head
Fusion Behaviour / Version 4.2.10

Test Conditions

Order	: HDPErGO0.20wt	Speed	:	50	1/min
Operator	: woh	Mixer Temp.	:	150	°C
Date	: 6/7/2015 16:48	Start Temp.	:	146	°C
Drive Unit	: Plastograph EC	Meas. Range	:	100	Nm
Mixer	: W 50 EHT - 3 Zones	Damping	:	0	
Loading Chute	: Manual + 5 kg	Test Time	:	10.00	min
Sample	: HDPErGO0.20wt	Sample Mass	:	40.0	g
Additive	: rGO0.20wt	Code Number	:		

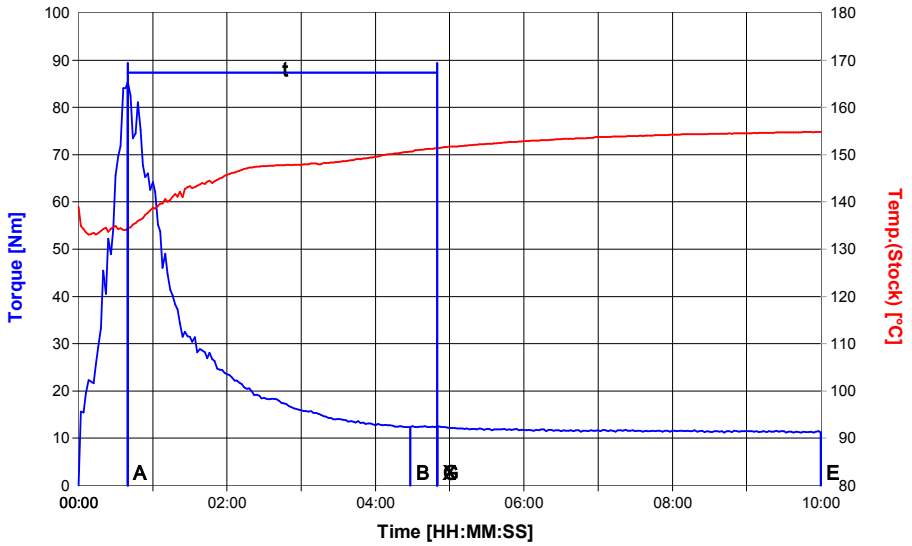

Name		Time [HH:MM:SS]	Torque [Nm]	Stock Temp. [°C]
Loading Peak	A	00:00:40	85.4	134
Minimum	B	00:04:28	12.4	151
Inflection Point	G	00:04:50	12.5	151
Maximum	X	00:04:50	12.5	151
End	E	00:10:00	11.2	155

Integration / Energy

Loading Peak	to Minimum	A - B	13.2	[kNm]
Minimum	to Maximum	B - X	0.7	[kNm]
Maximum	to End	X - E	8.2	[kNm]
Loading Peak	to Maximum	A - X	13.9	[kNm]
Loading Peak	to End (W)	A - E	22.1	[kNm]
Specific Energy(W/Sample Mass)			552.6	[kNm/kg]
Gelation Area above B		B - X	0.1	[kNm]

Results

Fusion Time t	A - X	00:04:10	[HH:MM:SS]
Gelation Speed v		-0.7	[Nm/min]